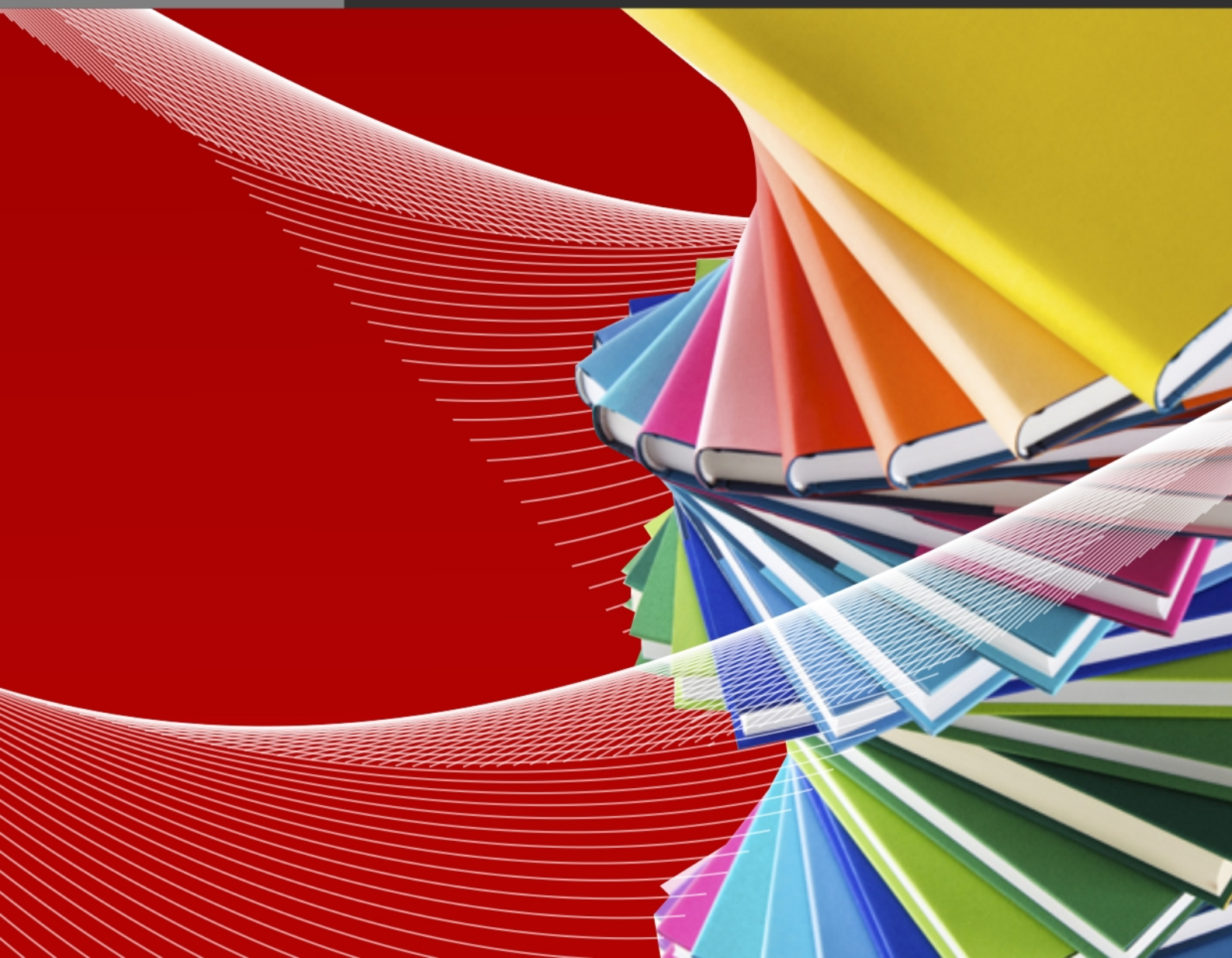![University of Macau logo]

澳 門 大 學
UNIVERSIDADE DE MACAU
UNIVERSITY OF MACAU

Outstanding Academic Papers by Students
學 生 優 秀 作 品

Analysis of Some Geometrically Nonlinear Catenary Structures under Static Loads

by

REN CHENJIE

Final Year Project Report submitted in partial fulfillment

of the requirement of the Degree of

Bachelor of Science in Civil Engineering

2016/2017

Faculty of Science and Technology
University of Macau

DECLARATION

I declare that the project report here submitted is original except for the source materials explicitly acknowledged and that this report as a whole, or any part of this report has not been previously and concurrently submitted for any other degree or award at the University of Macau or other institutions.

I also acknowledge that I am aware of the Rules on Handling Student Academic Dishonesty and the Regulations of the Student Discipline of the University of Macau.

Signature : _REN CHENJIE_

Name : _REN CHENJIE_
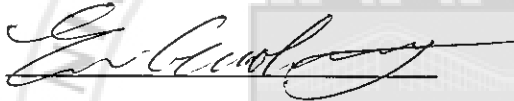
Student ID : _D-B3-2714-1_

Date : _2017. 5. 18_

APPROVAL FOR SUBMISSION

This project report entitled "**Analysis of Some Geometrically Nonlinear Catenary Structures under Static Loads**" was prepared by REN CHENJIE in partial fulfillment of the requirements for the degree of Bachelor of Science in Civil Engineering at the University of Macau.

Endorsed by,

Signature   :

Supervisor   : Prof. Er Guokang

ACKNOWLEDGEMENTS

I would like to first express my deepest gratitude to my supervisor, Prof. Er Guokang, who gave me the opportunity to do this wonderful project on the topic "Analysis of Some Geometrically Nonlinear Catenary Structures under Static Loads", while providing me a lot of valuable suggestions on the improvement of the thesis.

Secondly, I would like to express my special thanks to all the staffs in Faculty of Science and Technology for their hard work on spreading knowledge to us in the past four years, which enables me to finish this project properly.

Last but not least, I would also like to express my sincere appreciation to my parents and my friends, especially to Dr. Wang Kun, for their consistent encouragement and help on the finish of this thesis.
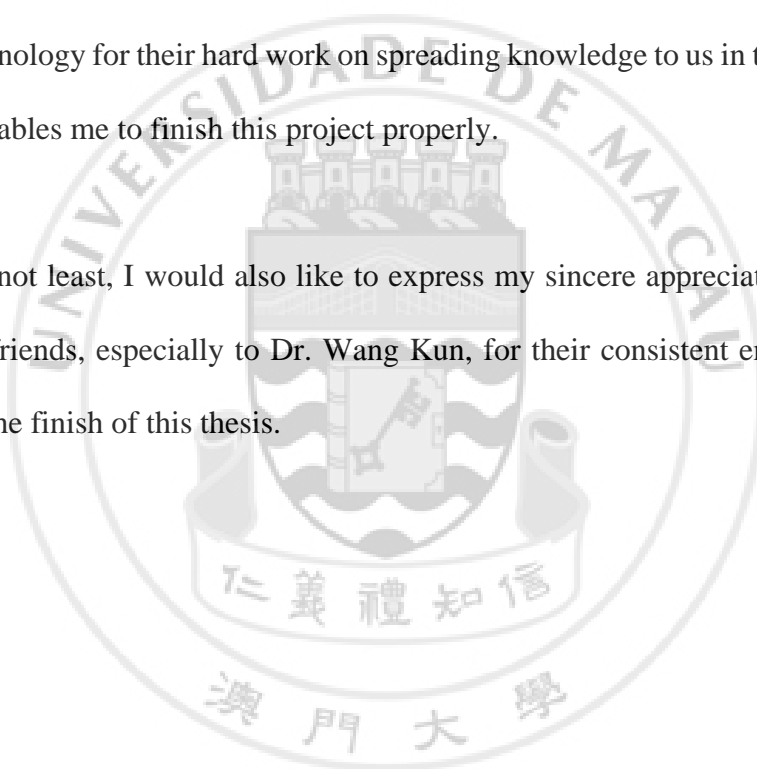
ABSTRACT

The behavior of a cable truss is generally considered as being analytically nonlinear. This thesis follows Irvine's procedures to derive the nonlinear and linear analytical solutions of cable truss systems, taking into account the geometry, pretension, boundary condition and temperature difference. After the final closed-form solution is achieved, the resultant increase in horizontal component of cable force in both top and bottom chords of a cable truss can be solved correspondingly, with which the deflection at midspan of the cable truss can be further figured out. This kind of work is done by transforming the solution into computer program. With the help of numerical method, it is found there is obvious difference between the results of nonlinear solution and linear solution. Besides, 10 different cases are assumed and solved to see the effect that parameters related to the solutions will have on the difference of the result from those two kinds of approaches, in which the considered parameters include the span-to-sag ratio, span-to-camber ratio, pretension in chords and temperature difference in both top and bottom chords. It is found the difference of resultant horizontal force in bottom chord for a biconcave cable truss from the two approaches and the difference of resultant force in top chord for a biconvex cable truss from the two approaches are most sensitive to the change of any of the considered parameters. However, it should be noted all the results and the conclusions are obtained within a limited range.

TABLE OF CONTENTS

LIST OF FIGURES

LIST OF TABLES

LIST OF SYMBOLS

A_b, A_t = cables cross-sectinal areas of bottom and top chords, respectively;

B_b, B_t = parameters characterizing boundary conditions at supports of bottom and top cables, respectively, in longitudinal direction;

c = camber of stabilizing cable;

ds_b, ds_t = original lengths of bottom and top elements, respectively;

E_b, E_t = modulus of elasticity of bottom and top chords, respectively;

$f_{xb}(0), f_{xb}(l), f_{xt}(0), f_{xt}(l)$

= horizontal support flexibilities of bottom and top ends of truss;

H_{0b}, H_{0t} = horizontal components of pretensions in bottom and top chords, respectively;

$L_{eb}, L_{et}, L_{Tb}, L_{Tt}$

= members characterizing lengths of unloaded cables;

l = span of cable truss;

Q = shear force;

q = vertical uniformly distributed load;

s = sag of carrying cable;

T_0, T = initial and design temperatures, respectively;

$u_b(0), u_b(l), u_t(0), u_t(l)$

= longitudinal movements of bottom and top supports, respectivley;

w = additional vertical deflection;

z_b, z_t = initial profiles of bottom and top chords, respectively;

α = coefficient of temperature expansion;

$\Delta H_b, \Delta H_t$ = additional horizontal components of cable tension in bottom and top chords, respectively;

$\Delta T_b, \Delta T_t$ = uniform temperature difference;

$\varepsilon_{eb}, \varepsilon_{et}$ = elastic strain in bottom and top chords, respectively;

$\varepsilon_{Tb}, \varepsilon_{Tt}$ = temperature strain in bottom and top chords, respectively.

CHAPTER 1 INTRODUCTION

1.1 Background

Cable trusses, as one of the suspension systems, are becoming quite popular nowadays since it can be constructed rapidly and can easily span over a large distance or area. Also, with the development of production for steel cable strands and the availability of numerical programs to handle more complex analysis of cable configurations, cable truss tends to show its advantage in cost compared with other types of constructions.

Due to the light weight and flexibility of cable trusses, large displacements can occur when being under loadings. Since the stresses in cables are related to the deflection, the overall stiffness of the structure will change as the geometry changes. So cable trusses are generally regarded as geometrically nonlinear structures. Although some techniques like prestressing are usually used to make sure the deflection is well under control, nonlinear analysis is still preferred to allow for more accurate results.

1.2 Basement

This thesis is mainly based on the theories and approaches proposed by Irvine (1981). For simplicity, he assumed the cables to be flat with relatively low sag, which is usually true for structural purpose. Some detailed theories were then derived to provide explicit, consistent methods for finding static response to applied loads accurated to the third order of small quantities.

He first set up a profile equation of the cable considering the unit weight and the resulting horizontal component of cable tension. Some terms were ignored in comparison to unity due to the overall flat profile as assumed. Cable length equation

was subsequently derived taking into account the sag and the effects of cable stretch, together with the sag equation at the midspan of the cable before any load is applied.

Next, a point load, as example, was added to the cable to explain the response. The shear force equilibrium inside the cable after the point load is applied was checked and further integrated to give the equations for the additional vertical deflection. The differential equations of cable elements before and after the load is applied were illustrated and combined with Hooke's law to relate the changes in cable tension to the changes in cable geometry. After necessary transformations and integrations, a dimensionless cubic equation containing only one unknown, the increment in the horizontal component of cable tension, was yield as the final nonlinear solution. In addition to this, Irvine (1981) also provided linearized solutions for the point load problem. He neglected all second-order terms that appear in the differential equations of equilibrium and in the cable equation, which resulted in the removal of some terms occurred in the nonlinear solution. At the end, as comparison, he spent some words discussing the cases of which linearized solutions were valid.

The derivation of responses to a uniformly distributed load was quite similar to the one for a point load, only with some formations of equations changed.

In this thesis, similar procedures of derivation will be performed, but for a suspended cable truss case with its self-weight ignored.

1.3 Overview

In this thesis, the nonlinear analytical approach for a single suspended cable proposed by Irvine (1981) is adopted and extended to the cable truss case to give the corresponding nonlinear analytical solution under a uniformly distributed load, which will be further compared to the linear one to see the difference. In the coming literature

review part, a detailed review of cable-related and cable truss-related works will be performed with some comments. The procedures to derive the final nonlinear and linear solutions of this thesis will be clearly described in the next methodology part. For the results and discussion part, some related parameter values will be assumed in different cases and put into the solutions obtained for further analysis, so as to find out the effect each parameter will have on the difference of results of nonlinear and linear approaches. In the final conclusion and recommendations part, some important points in the thesis will be restated to relate all the works together, and some recommendations will also be provided on the further works that can be practiced based on this thesis.

CHAPTER 2 LITERATURE REVIEW

2.1 Linear Approach

To analyze cable trusses, Zetlin (1963) proposed a linear approximate equation to calculate the force and displacement under uniformly distributed loads over the entire span. As this equation is derived based on the initial geometry of the cable truss, deflection after loads are applied has no effect on the force result, which may cause significant error when large deflection occurs. Mollmann (1970) suggested an approximate equation similar to Zetlin's with more consideration on unsymmetrical loadings, flexible supports and temperature changes. Some other methods (Thornton and Birnstiel 1967; Krishna and Sparkes 1968; Buchholdt 1969; Schleyer 1969) can be found to analyze cable trusses using mostly linear models and iterative method. However, these methods are still not completed since many structural parameters are ignored, such as support flexibility, cable size, prestressing force, sag-to-span ratio, etc., all of which could have effects on the final stress and deflection of the cable truss. Besides, based on linear static analytical model, simple approaches for preliminary design of cable structures are discussed in further works (Baron and Venkatesan 1971; Urelius and Fowler 1974; Moskalev 1980; Kadlcak 1995; Buchholdt 1999).

2.2 Nonlinear Approach

As mentioned before, nonlinear analysis is still preferred for the cable truss in some cases. Most of recent works (Jayaraman and Knudson 1981; Kmet 1994; Levy and Spillers 1995; Talvik 2001; Gasparini and Gautam 2002) related to this kind of analysis are based on the finite element method, which will be simply introduced later, and the solving of resulting nonlinear algebraic equations by numerical methods. However, only a few published analytical studies focus on the nonlinear solutions. Irvine (1981)

4

proposed some detailed procedures to nonlinearly relate the physical properties and geometrical quantities of the cable to the final deflection and the inside stress, together with a simple linear approach. By transforming nonlinear loading parameters of cable trusses into linear ones, Rakowski (1983) tried to solve nonlinear analytical solutions by linear method. Kassimali and Parsi-Feraidoonian (1987) studied some nonlinear behaviors of cable trusses to figure out the ultimate strength of prestressed cables, taking into account the effects of displacement, material properties, etc.

2.3 Numerical Approach

Numerical method is also a popular approach to analyze the cable truss, as complex mathematical problems can arise during the analysis. There are mainly two ways to analyze cable members numerically. One is based on the expressions of elastic catenary, of which the theory was first proposed by O'Brien and Francis (1964). Peyrot and Goulois (1978) later presented the corresponding elastic catenary element. More related developments of elastic catenary can be found in other works (Jayaraman and Knudson 1981; Wang et al. 2003; Andreu et al. 2006; Yang and Tsay 2007; Such et al. 2009). The other is based on finite element technique, in which three different types of elements are mainly adopted. The first type is two-node element, or straight element. This is the most common one and was developed in several works (Argyris and Scharpf 1972; Gambhir and Batchelor 1979; Ozdemir 1979; Broughton and Ndumbaro 1994). Some studies (Coyette and Guisset 1988; Ali and Abdel-Ghaffar 1995; Chen et al. 2010) also used the second type, multi-node element, to avoid using many two-node elements and to give more accurate results. The last type is curved element with rotational degrees of freedom. Gambhir and Batchelor (1977) proposed this type of element to take the continuity of slopes into consideration.

CHAPTER 3 METHODOLOGY

3.1 General Analytical Model

The geometries of the cable trusses considered in this thesis are shown below, with biconcave one in Fig. 3.1 and biconvex one in Fig. 3.2. The profiles of the top and bottom chords are determined by assuming them as parabolas with three points known and are calculated as

$$z_t = 4(d_t - b_t)\frac{x}{l}\left(1 - \frac{x}{l}\right) + b_t$$

$$z_b = 4(d_b - b_b)\frac{x}{l}\left(1 - \frac{x}{l}\right) + b_b$$

(3.1)

where $l =$ span of the cable truss, m. For the biconcave truss, sag of the top cable and camber of the bottom cable are defined as $s = b_t - d_t$ and $c = b_b - d_b$ respectively. For the biconvex truss, sag of the bottom cable and camber of the top cable are defined as $s = d_b - b_b$ and $c = d_t - b_t$ respectively.

Fig. 3.1. Geometry for biconcave cable truss

6
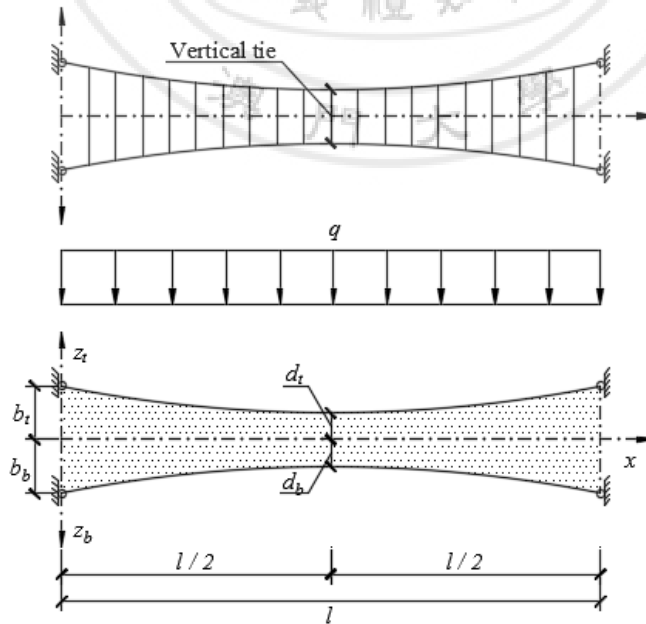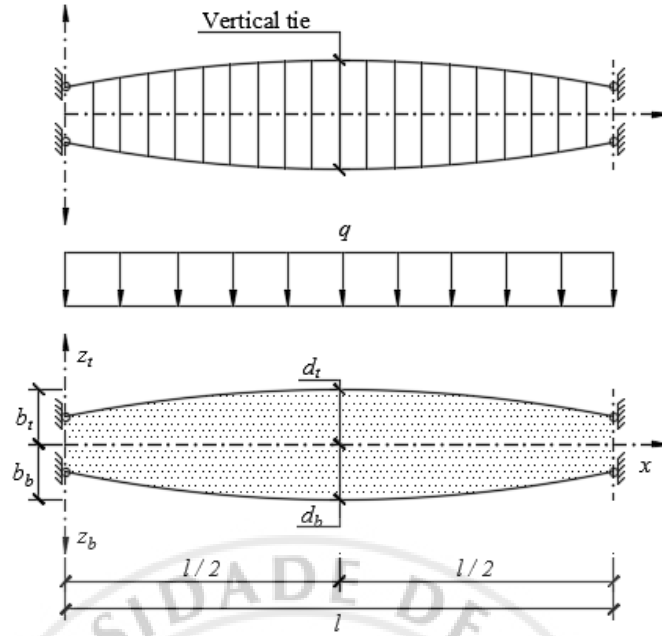
Fig. 3.2. Geometry for biconvex cable truss

For convenience, the subsequent analysis will be performed under the following assumptions: (1) Cables are totally flexible so that only tension occurs. (2) All the small weight of the cables and the spacers will not be considered. (3) The slopes of the chords remain small when experiencing deformation. (4) Vertical spacers or ties of the trusses will be replaced by a continuous diaphragm with inextensible vertical elements, as shown in the figures. (5) The small longitudinal movements of the chords due to the vertical deflection will occur freely.

The derivation of the final solution will be performed with the biconvex cable truss under uniformly distributed load over the entire span, while the example results will be obtained considering both biconcave truss and biconvex truss since the solution can be applied equally to both types.

3.2 Nonlinear Analytical Solution

Since the considered biconvex cable truss experiences a uniformly distributed load q on the entire span (see Fig. 3.3), based on the knowledge of structure analysis, the shear force at cross section x from the support is $Q = ql/2(1 - 2x/l)$. Referring to Irvine (1981), the vertical equilibrium at cross section further requires that

$$\left(H_{0b} + \Delta H_b\right)\frac{d\left(z_b + w\right)}{dx} - \left(H_{0t} - \Delta H_t\right)\frac{d\left(z_t - w\right)}{dx} = \frac{ql}{2}\left(1 - \frac{2x}{l}\right) \qquad (3.2)$$

where H_{0b} and H_{0t} = horizontal components of the pretensions in the bottom and top chords, kN; ΔH_b and ΔH_t = additional horizontal components of cable tension due to the applied load, kN; z_b and z_t = initial profiles of the chords given by Eq. (3.1), m; w = additional vertical deflection, m. The internal equilibrium of the unloaded truss, expressed as $H_{0b} dz_b / dx = H_{0t} dz_t / dx$, can be obtained by picking out ΔH_b, ΔH_t, w and shear force in Eq. (3.2). Taking this into account, Eq. (3.2) can be simplified into
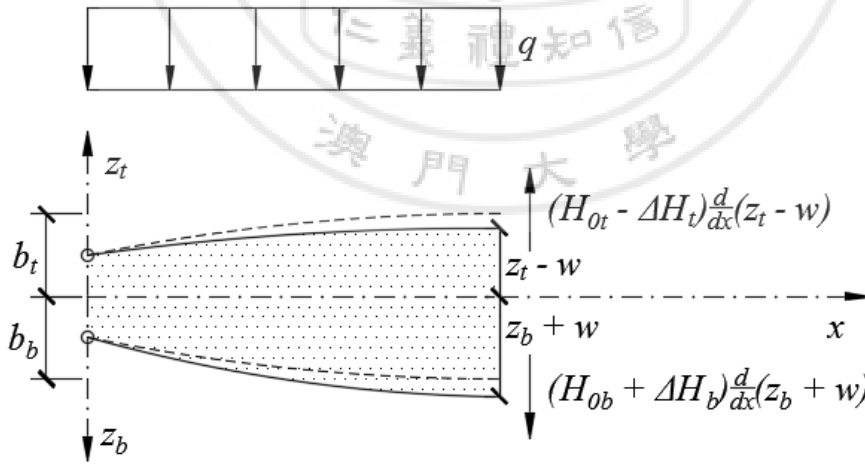
Fig. 3.3. Vertical equilibrium of biconvex cable truss
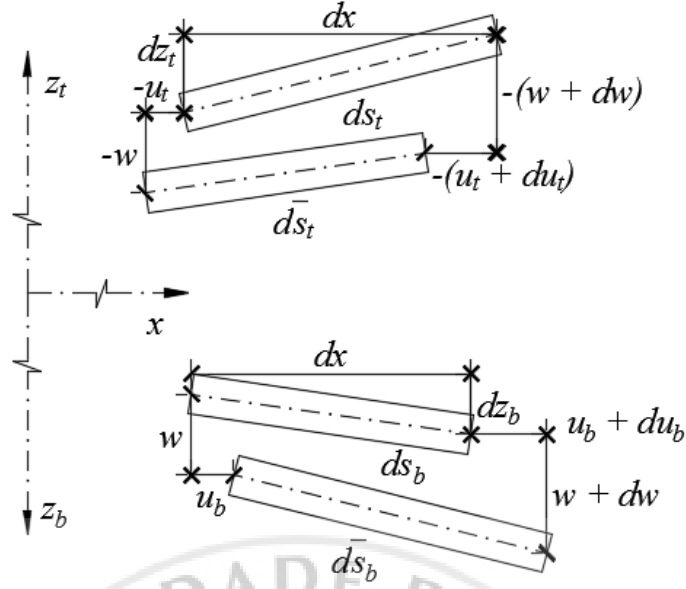
Fig. 3.4. Displacements of elements of bottom and top cables in biconvex truss

$$\left(H_{0b}+\Delta H_{b}+H_{0t}-\Delta H_{t}\right)\frac{dw}{dx}+\Delta H_{b}\frac{dz_{b}}{dx}+\Delta H_{t}\frac{dz_{t}}{dx}=\frac{ql}{2}\left(1-\frac{2x}{l}\right) \tag{3.3}$$

After the boundary conditions being applied, Eq. (3.3) can be integrated directly to obtain the overall vertical deflection equation for biconvex cable truss

$$w=\frac{1}{H_{0b}+\Delta H_{b}+H_{0t}-\Delta H_{t}}\left[\frac{ql}{2}x\left(1-\frac{x}{l}\right)-4\Delta H_{b}\left(d_{b}-b_{b}\right)\left(\frac{x}{l}-\frac{x^{2}}{l^{2}}\right)\right.$$

$$\left.-4\Delta H_{t}\left(d_{t}-b_{t}\right)\left(\frac{x}{l}-\frac{x^{2}}{l^{2}}\right)\right] \tag{3.4}$$

As ΔH_{b} and ΔH_{t} are necessary for the final solution, Hooke's law is made use of to find the relationship between the changes in cable tensions and the displacements of chords. For a biconvex truss, the geometry of these displacements are shown in Fig. 3.4. Considering ds_{b} and ds_{t} as the original lengths of the bottom and top elements, and $d\bar{s}_{b}$ and $d\bar{s}_{t}$ as their new length, then $ds_{b}^{2}=dx^{2}+dz_{b}^{2}$, $d\bar{s}_{b}^{2}=(dx+du_{b})^{2}+(dz_{b}+dw)^{2}$, $ds_{t}^{2}=dx^{2}+dz_{t}^{2}$, and $d\bar{s}_{t}^{2}=(dx-du_{t})^{2}+(dz_{t}-dw)^{2}$, where u_{b} and $u_{t}=$ longitudinal

9

displacements of the elements, m. For flat-sag cables, the fractional changes in their lengths (use bottom chord as example) can be first derived as

$$
\frac{d\bar{s}_b - ds_b}{ds_b} = \sqrt{\frac{(dx + du_b)^2 + (dz_b + dw)^2}{ds_b^2}} - 1
$$

$$
= \sqrt{\frac{dx^2 + dz_b^2 + 2du_b dx + 2dw dz_b + dw^2 + du_b^2}{ds_b^2}} - 1 \tag{3.5}
$$

$$
= \sqrt{1 + 2\frac{du_b}{ds_b}\frac{dx}{ds_b} + 2\frac{dw}{ds_b}\frac{dz_b}{ds_b} + \left(\frac{dw}{ds_b}\right)^2 + \left(\frac{du_b}{ds_b}\right)^2} - 1
$$

Based on Taylor series, function in the form of $f(x) = \sqrt{1+x}$ can be corrected to the second item to give $f(x) = T(0) = 1 + x/2$, thus Eq. (3.5) can be transformed into

$$
\frac{d\bar{s}_b - ds_b}{ds_b} = 1 + \frac{1}{2}\left[2\frac{du_b}{ds_b}\frac{dx}{ds_b} + 2\frac{dw}{ds_b}\frac{dz_b}{ds_b} + \left(\frac{dw}{ds_b}\right)^2 + \left(\frac{du_b}{ds_b}\right)^2\right] - 1
$$

$$
= \frac{du_b}{ds_b}\frac{dx}{ds_b} + \frac{dw}{ds_b}\frac{dz_b}{ds_b} + \frac{1}{2}\left(\frac{dw}{ds_b}\right)^2 + \frac{1}{2}\left(\frac{du_b}{ds_b}\right)^2 \tag{3.6}
$$

The term $\frac{1}{2}(du_b/ds_b)^2$ in Eq. (3.6) is ignored in the following analysis due to its relative small value compared to the others. The fractional change in length for the top chord can be derived in the same manner and together gives

$$
\frac{d\bar{s}_b - ds_b}{ds_b} = \frac{du_b}{ds_b}\frac{dx}{ds_b} + \frac{dw}{ds_b}\frac{dz_b}{ds_b} + \frac{1}{2}\left(\frac{dw}{ds_b}\right)^2
$$

$$
\frac{d\bar{s}_t - ds_t}{ds_t} = \frac{du_t}{ds_t}\frac{dx}{ds_t} + \frac{dw}{ds_t}\frac{dz_t}{ds_t} - \frac{1}{2}\left(\frac{dw}{ds_t}\right)^2 \tag{3.7}
$$

According to Hooke's law, here requires that

$$
\frac{d\bar{s}_b - ds_b}{ds_b} = \frac{\Delta H_b}{E_b A_b}\frac{ds_b}{dx}
$$

$$
\frac{d\bar{s}_t - ds_t}{ds_t} = \frac{\Delta H_t}{E_t A_t}\frac{ds_t}{dx} \tag{3.8}
$$

10

where E_b and E_t = moduli of elasticity of the bottom and top chords, kN m^{-2}; and A_b and A_t = cross-sectional areas of the cable chords, m^2.

If the effects of a uniform temperature change of $\Delta T_b = T_b - T_{0b}$ and/or $\Delta T_t = T_t - T_{0t}$ (where T and T_0 = the design and initial temperatures, ℃ or K) are considered, terms $\varepsilon_{Tb} = \alpha \Delta T_b$ and $\varepsilon_{Tt} = \alpha \Delta T_t$ need to be added to the elemental equations, where α = coefficient of expansion, ℃$^{-1}$ or K^{-1}. Based on Eq. (3.7) and Eq. (3.8), cable equations for the bottom and top elements can be expressed as

$$\frac{\Delta H_b}{E_b A_b}\frac{ds_b}{dx} + \alpha \Delta T_b = \frac{du_b}{ds_b}\frac{dx}{ds_b} + \frac{dw}{ds_b}\frac{dz_b}{ds_b} + \frac{1}{2}\left(\frac{dw}{ds_b}\right)^2$$

$$\frac{\Delta H_t}{E_t A_t}\frac{ds_t}{dx} + \alpha \Delta T_t = \frac{du_t}{ds_t}\frac{dx}{ds_t} + \frac{dw}{ds_t}\frac{dz_t}{ds_t} - \frac{1}{2}\left(\frac{dw}{ds_t}\right)^2$$

(3.9)

After respective multiplication of Eq. (3.9) by $(ds_b / dx)^2$ and $(ds_t / dx)^2$, one obtains

$$\frac{\Delta H_b}{E_b A_b}\left(\frac{ds_b}{dx}\right)^3 + \alpha \Delta T_b\left(\frac{ds_b}{dx}\right)^2 = \frac{du_b}{dx} + \frac{dw}{dx}\frac{dz_b}{dx} + \frac{1}{2}\left(\frac{dw}{dx}\right)^2$$

$$\frac{\Delta H_t}{E_t A_t}\left(\frac{ds_t}{dx}\right)^3 + \alpha \Delta T_t\left(\frac{ds_t}{dx}\right)^2 = \frac{du_t}{dx} + \frac{dw}{dx}\frac{dz_t}{dx} - \frac{1}{2}\left(\frac{dw}{dx}\right)^2$$

(3.10)

Eq. (3.10) can be further integrated to give the form

$$\frac{\Delta H_b L_{eb}}{E_b A_b} + \alpha \Delta T_b L_{Tb} = u_b(l) - u_b(0) + \int_0^l \left(\frac{dw}{dx}\frac{dz_b}{dx}\right)dx + \frac{1}{2}\int_0^l \left(\frac{dw}{dx}\right)^2 dx$$

$$\frac{\Delta H_t L_{et}}{E_t A_t} + \alpha \Delta T_t L_{Tt} = u_t(l) - u_t(0) + \int_0^l \left(\frac{dw}{dx}\frac{dz_t}{dx}\right)dx - \frac{1}{2}\int_0^l \left(\frac{dw}{dx}\right)^2 dx$$

(3.11)

where $u_b(l)$ and $u_b(0)$ and/or $u_t(l)$ and $u_t(0)$ = longitudinal movements of the bottom and top supports, respectively, m. The left side members L_{Tb} and L_{Tt} of Eq. (3.11) can be determined directly, while L_{eb} and L_{et} can be calculated using Taylor series and corrected to the second item, of which the procedure is similar to the one from Eq. (3.5)

11

to Eq. (3.6). These members characterize the lengths of the unloaded cables and are given by

$$L_{Tb,t} = \int_0^l \left(\frac{ds_{b,t}}{dx} \right)^2 dx$$

$$= \int_0^l \left[1 + \left(\frac{dz_{b,t}}{dx} \right)^2 \right] dx$$

$$= \int_0^l dx + 16 \left(\frac{d_{b,t} - b_{b,t}}{l} \right)^2 \int_0^l \left(1 - \frac{2x}{l} \right)^2 dx$$

$$= l \left[1 + \frac{16}{3} \left(\frac{d_{b,t} - b_{b,t}}{l} \right)^2 \right]$$

$$L_{eb,t} = \int_0^l \left(\frac{ds_{b,t}}{dx} \right)^3 dx$$

$$= \int_0^l \left[1 + \left(\frac{dz_{b,t}}{dx} \right)^2 \right]^{\frac{3}{2}} dx$$

$$= \int_0^l \left[1 + \frac{3}{2} \left(\frac{dz_{b,t}}{dx} \right)^2 \right] dx \tag{3.12}$$

$$= l \left[1 + 8 \left(\frac{d_{b,t} - b_{b,t}}{l} \right)^2 \right]$$

where the terms are defined in Fig. 3.1 and Fig. 3.2.

Because dw/dz is continuous along the span, the integral terms on the right side of Eq. (3.11) can be evaluated by integration by parts as

$$\int_0^l \left(\frac{dw}{dx} \frac{dz_{b,t}}{dx} \right) dx = \left[w \frac{dz_{b,t}}{dx} \right]_0^l - \int_0^l \frac{d^2 z_{b,t}}{dx^2} w dx = -\int_0^l \frac{d^2 z_{b,t}}{dx^2} w dx$$

$$\frac{1}{2} \int_0^l \left(\frac{dw}{dx} \right)^2 dx = \frac{1}{2} \left[w \frac{dw}{dx} \right]_0^l - \frac{1}{2} \int_0^l \frac{d^2 w}{dx^2} w dx = -\frac{1}{2} \int_0^l \frac{d^2 w}{dx^2} w dx \tag{3.13}$$

With Eq. (3.13) derived, Eq. (3.11) can be rewritten as

$$\frac{\Delta H_b L_{eb}}{E_b A_b} + \alpha \Delta T_b L_{Tb} = -\int_0^l \frac{d^2 z_b}{dx^2} w \, dx - \frac{1}{2} \int_0^l \frac{d^2 w}{dx^2} w \, dx + B_b$$

$$\frac{\Delta H_t L_{et}}{E_t A_t} + \alpha \Delta T_t L_{Tt} = -\int_0^l \frac{d^2 z_t}{dx^2} w \, dx + \frac{1}{2} \int_0^l \frac{d^2 w}{dx^2} w \, dx + B_t$$

(3.14)

where parameters B_b and B_t characterize the boundary conditions at the supports of the bottom and top cables, respectively, in the longitudinal direction. For unmovable supports $B_b = 0$ and $B_t = 0$. For movable supports, if horizontal movements occurs at the corresponding ends of the truss, then $B_b = u_b(l) - u_b(0)$ and $B_t = u_t(l) - u_t(0)$. For elastic supports in the horizontal direction $B_b = f_{xb}(0) + f_{xb}(l)$ and $B_t = f_{xt}(0) + f_{xt}(l)$, where the horizontal supports flexibilities of f_{xb} and/or f_{xt} occur at corresponding ends of the truss.

Substituting Eq. (3.1), Eq. (3.4) and Eq. (3.12) into Eq. (3.14) and performing the necessary integration, a coupled system of cubic cable equations for ΔH_b and ΔH_t can be found. This nonlinear closed-form solution can be put directly into software *MATLAB 2016b* to obtain the answers with corresponding values of parameters given and the embedded *fsolve* function. The program code will be given in the appendix.

3.3 Linear Analytical Solution

The model is linearized by neglecting all second-order terms that appear in the differential equations of equilibrium and in the cable equation. This requires the removal of the term $\Delta H_b dw/dx$ and $\Delta H_t dw/dx$ from Eq. (3.3) and $\frac{1}{2}\int_0^l (dw/dx)^2 dx$ from Eq. (3.11). As a consequence the deflection changes into

13

$$w = \frac{1}{H_{0b} + H_{0t}} \left[\frac{ql}{2} x \left(1 - \frac{x}{l}\right) - 4\Delta H_b \left(d_b - b_b\right)\left(\frac{x}{l} - \frac{x^2}{l^2}\right) \right.$$

$$\left. -4\Delta H_t \left(d_t - b_t\right)\left(\frac{x}{l} - \frac{x^2}{l^2}\right) \right] \qquad (3.15)$$

and the final cable equations become

$$\frac{\Delta H_b L_{eb}}{E_b A_b} + \alpha \Delta T_b L_{Tb} = -\int_0^l \frac{d^2 z_b}{dx^2} w\, dx + B_b$$

$$\frac{\Delta H_t L_{et}}{E_t A_t} + \alpha \Delta T_t L_{Tt} = -\int_0^l \frac{d^2 z_t}{dx^2} w\, dx + B_t \qquad (3.16)$$

Substituting Eq. (3.1), Eq. (3.12) and Eq. (3.15) into Eq. (3.16) and performing necessary integration, a coupled system of linear cable equations for ΔH_b and ΔH_t can be obtained. Similarly, these equations can be put directly into *MATLAB 2016b* to get the answers. The corresponding program code will also be shown in the appendix.

CHAPTER 4 RESULTS AND DISCUSSION

After the nonlinear and linear solutions being derived, some cases will be studied to further discuss about the effects of parameters in solutions on the final results.

4.1 Case Study 1: Different Span-to-sag Ratios of Top Chord for a Biconcave Cable Truss

Here a biconcave cable truss as shown in Fig. 3.1 is considered (Fig. 3.1 is put here again for convenience and better understanding, but will not be included in the list of figures), which have a span $l = 60$ m and cross-sectional areas of the bottom and top cables $A_b = 1.3 \times 10^{-3}$ m^2 and $A_t = 2.0 \times 10^{-3}$ m^2. Both cables has the moduli of elasticity of $E_b = E_t = 1.5 \times 10^8$ kN m^{-2}. A vertical uniformly distributed load $q = 10.0$ kN m^{-1} is applied over the entire span. In the closed-form analysis, the ties are replaced by a continuous diaphragm as described in the assumptions.
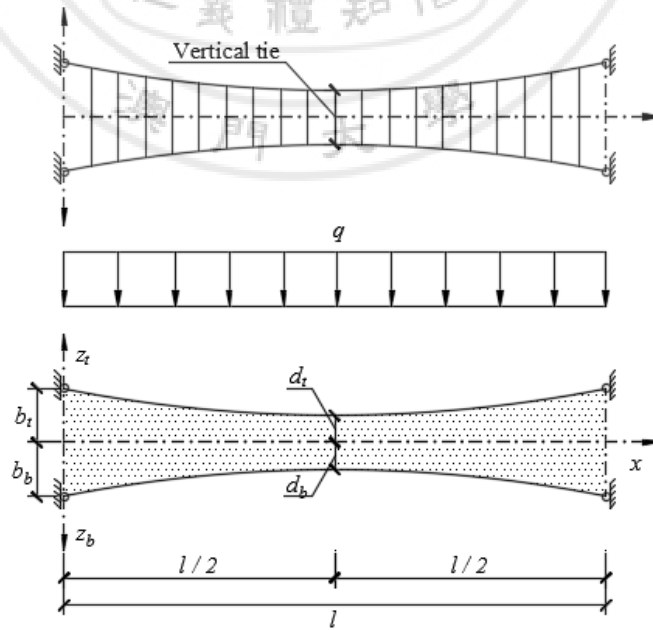
Fig. 3.1. Geometry for biconcave cable truss

Eight different span-to-sag ratios of the top carrying cable, $l/s = 7.5, 10, 12.5, 15,$ 17.5, 20, 22.5, and 25 are considered. The span-to-camber ratio of the bottom stabilizing cable is kept constant at $l/c = 25$ for all mentioned cases. The following data for the geometrical quantities are specified: $d_b = d_t = 0.5$ m, $b_b = 2.9$ m, and $b_t =$ 8.5, 6.5, 5.3, 4.5, 3.93, 3.5, 3.17, and 2.9 m, of which b_b is the sum of d_b and c while b_t is the sum of d_t and s. The initial horizontal component of pretension in the bottom chord is $H_{0b} = 600.0$ kN. Considering the internal equilibrium of the initial prestressed unloaded truss, the initial horizontal component of pretention in the top chord can be determined as $H_{0t} = H_{0b}c/s$.

To find out vertical deflections w in the midspan of the truss under applied load, $x = l/2$ is taken into Eq. (3.4) and Eq. (3.15) to give corresponding nonlinear form

$$w = \frac{1}{H_{0b} + \Delta H_b + H_{0t} - \Delta H_t} \left[\frac{ql^2}{8} - \Delta H_b \left(d_b - b_b \right) - \Delta H_t \left(d_t - b_t \right) \right] \tag{4.1}$$

and linear form

$$w = \frac{1}{H_{0b} + H_{0t}} \left[\frac{ql^2}{8} - \Delta H_b \left(d_b - b_b \right) - \Delta H_t \left(d_t - b_t \right) \right] \tag{4.2}$$

Table 4.1. Analytical results for Case Study 1

l/s	Nonlinear Solution, 10^3			Linear Solution, 10^3		
	H_b, kN	H_t, kN	w, mm	H_b, kN	H_t, kN	w, mm
7.5	0.4934	0.6867	0.1612	0.4873	0.6926	0.1647
10	0.4377	0.8705	0.2501	0.4219	0.8823	0.2601
12.5	0.3802	1.0264	0.3454	0.3492	1.0434	0.3663
15	0.3254	1.1575	0.439	0.2747	1.1758	0.4752
17.5	0.2773	1.2678	0.5299	0.2027	1.2818	0.5803
20	0.2344	1.3618	0.6121	0.1364	1.3653	0.6772
22.5	0.1975	1.4432	0.6859	0.0774	1.4308	0.7634
25	0.1662	1.515	0.7512	0.0264	1.4825	0.8379
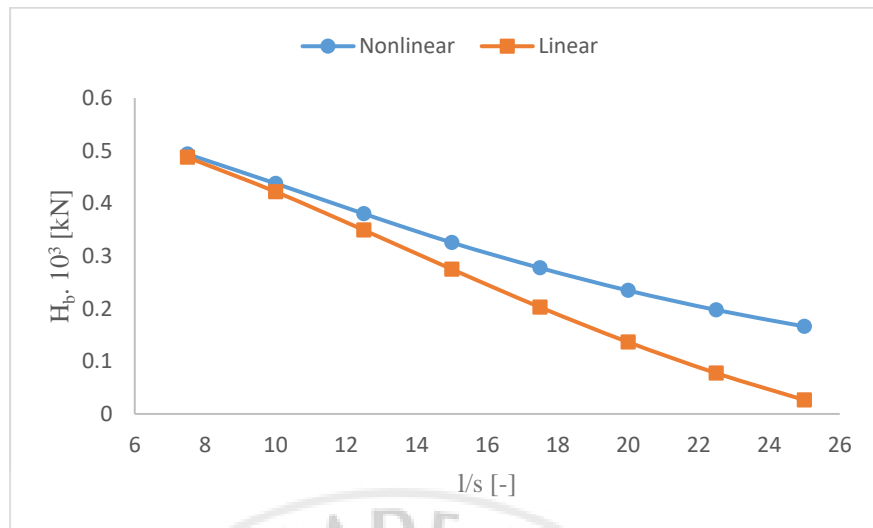
Fig. 4.1. Horizontal force in bottom chord vs. span-to-sag ratio in top chord for a

biconcave cable truss

Fig. 4.2. Horizontal force in top chord vs. span-to-sag ratio in top chord for a

biconcave cable truss

17

Fig. 4.3. Deflection at midspan vs. span-to-sag ratio in top chord for a biconcave cable truss

Horizontal components of cable forces in the bottom and top chords are calculated as $H_b = H_{0b} + \Delta H_b$ and $H_t = H_{0t} - \Delta H_t$, respectively, since the analytical solutions are derived for biconvex truss. Based on Eq. (4.1), Eq. (4.2) and the solutions derived before, the analytical results for H_b, H_t and deflection w are calculated and tabulated in Table 4.1. Graphs are made to better compare the results obtained from nonlinear and linear solution (see Fig. 4.1, Fig. 4.2 and Fig. 4.3), from which it is obviously shown that there are differences between the responses of the investigated cable trusses obtained from nonlinear and linear analyses. More detailed percent error of the results obtained by the linear solution compared to the nonlinear one is shown in Table 4.2 and is calculated based on the equation

$$\text{Percent Error} = \frac{\text{Nonlinear Result} - \text{Linear Result}}{\text{Nonlinear Result}} \times 100\% \qquad (4.3)$$

The positive percent errors indicate that the results of the linear solution are underestimated compared with the nonlinear one, while the negative values occur when the linear results are overestimated.

Table 4.2. Percent error of results for Case Study 1 (%)

l / s	7.5	10	12.5	15	17.5	20	22.5	25
H_b	1.2	3.6	8.2	15.6	26.9	41.8	60.8	84.1
H_t	-0.9	-1.4	-1.7	-1.6	-1.1	-0.3	0.9	2.1
w	-2.2	-4.0	-6.1	-8.2	-9.5	-10.6	-11.3	-11.5
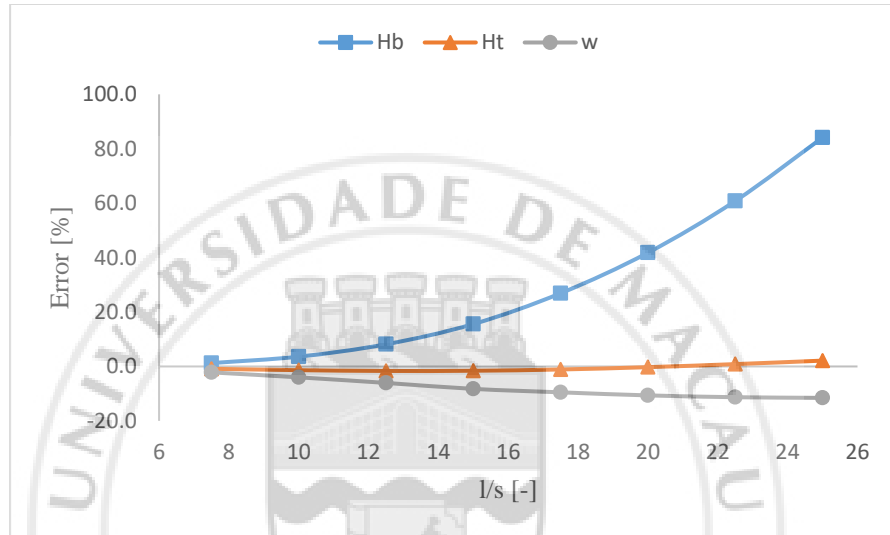
Fig. 4.4. Percent error of results vs. span-to-sag ratio in top chord for a biconcave

cable truss

The three curves shown in Fig. 4.4 illustrate that, with the span-to-sag ratio of the top chord increasing and all other parameters remain the same, the horizontal component of cable force in bottom chord obtained by linear solution becomes more and more underestimated, the deflection at midspan becomes somewhat more overestimated, while the difference of horizontal force in top chord obtained by two solutions remains almost the same.

4.2 Case Study 2: Different Span-to-camber Ratios of Bottom Chord for a Biconcave Cable Truss

Using the same model as Case Study 1, but this time the span-to-sag ratio of top chord is kept at $l/s = 25$, while eight different span-to-camber ratios of bottom chord, $l/c =$ 7.5, 10, 12.5, 15, 17.5, 20, 22.5, and 25 are adopted for a biconcave cable truss. Some values of related parameters are specified as: $d_b = d_t = 0.5$ m, $b_b = d_b + c$ and $b_t = d_t + s$ for corresponding cases.

Table 4.3. Analytical results for Case Study 2

| l/c	Nonlinear Solution, 10^3			Linear Solution, 10^3		
	H_b, kN	H_t, kN	w, mm	H_b, kN	H_t, kN	w, mm
7.5	0.1726	2.2355	0.214	0.1728	2.2224	0.2111
10	0.0989	1.8604	0.3208	0.0934	1.8324	0.3156
12.5	0.0624	1.6888	0.4261	0.0431	1.6446	0.4222
15	0.0562	1.6079	0.5202	0.0155	1.5517	0.5238
17.5	0.0717	1.5677	0.5998	0.0045	1.5069	0.6169
20	0.099	1.5443	0.6636	0.0051	1.4874	0.7002
22.5	0.1318	1.5285	0.7125	0.0133	1.4815	0.7736
25	0.1662	1.515	0.7512	0.0264	1.4825	0.8379
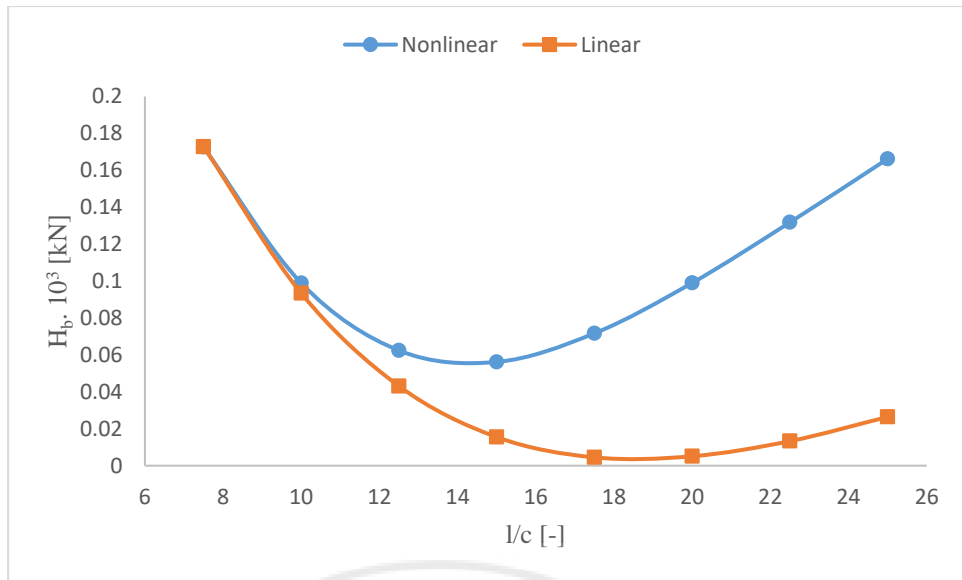
Fig. 4.5. Horizontal force in bottom chord vs. span-to-camber ratio in bottom chord
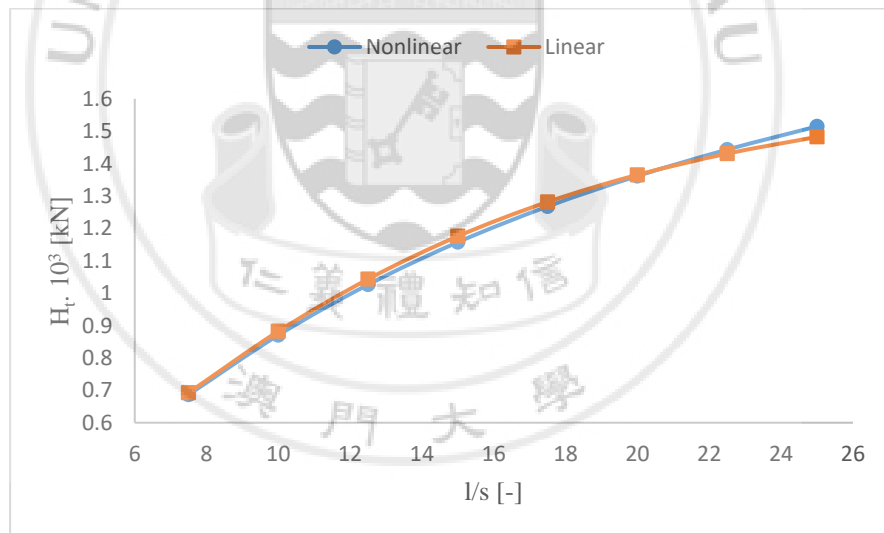
for a biconcave cable truss
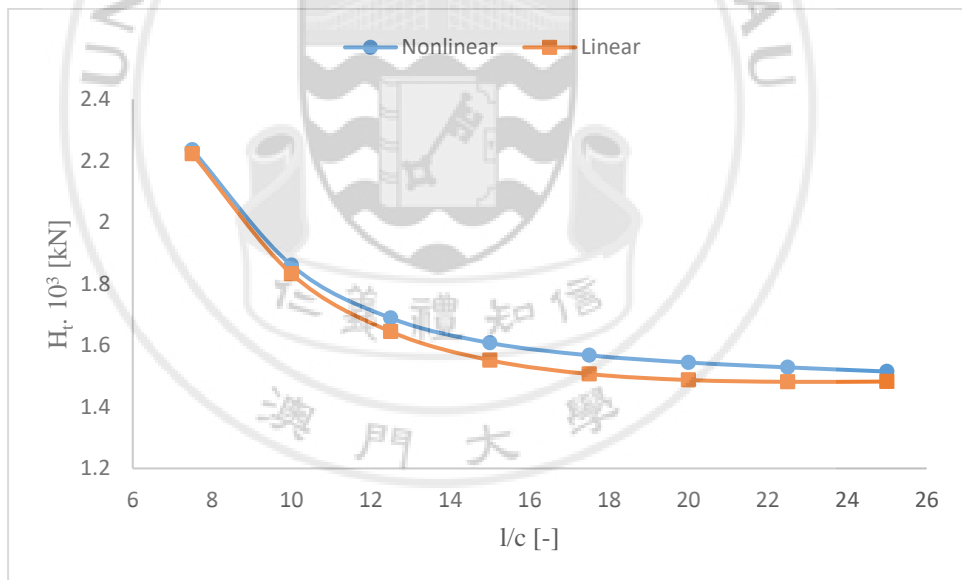
Fig. 4.6. Horizontal force in top chord vs. span-to-camber ratio in bottom chord for a

biconcave cable truss
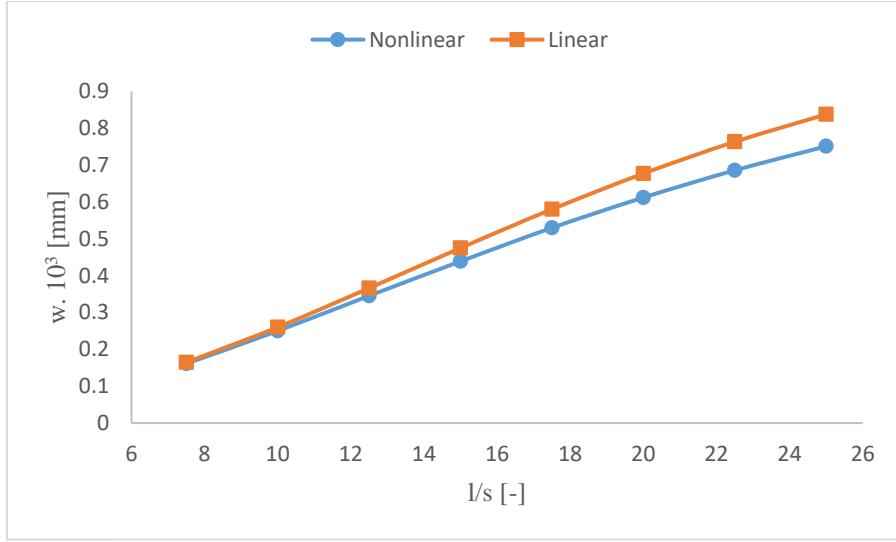
Fig. 4.7. Deflection at midspan vs. span-to-camber ratio in bottom chord for a

biconcave cable truss

Table 4.4. Percent error of results for Case Study 2 (%)

l / c	7.5	10	12.5	15	17.5	20	22.5	25
H_b	-0.1	5.6	30.9	72.4	93.7	94.8	89.9	84.1
H_t	0.6	1.5	2.6	3.5	3.9	3.7	3.1	2.1
w	1.4	1.6	0.9	-0.7	-2.9	-5.5	-8.6	-11.5
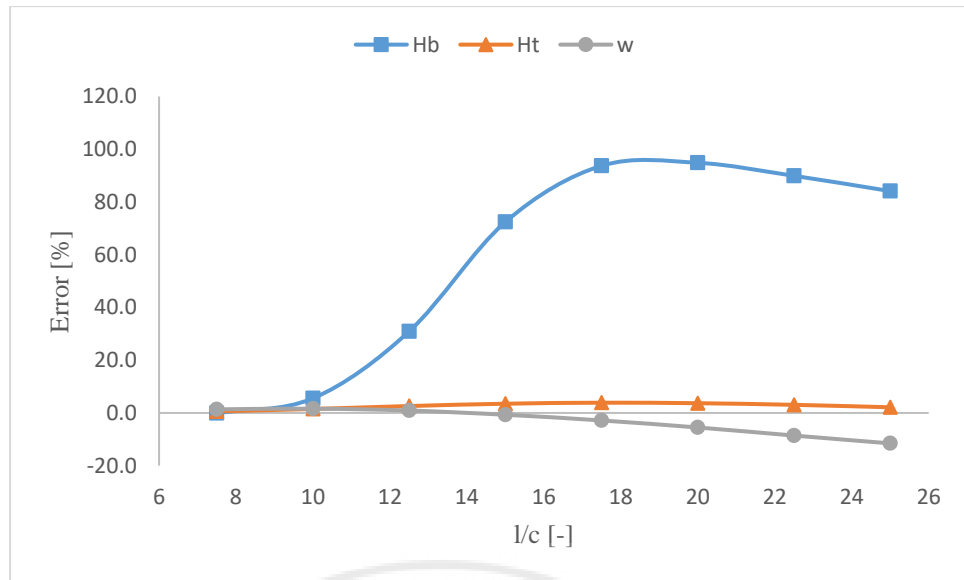
Fig. 4.8. Percent error of results vs. span-to-camber ratio in bottom chord for a biconcave cable truss

Same as Case Study 1, the analytical results in this case are tabulated in Table 4.3 and more straightforward observation can be obtained in Fig. 4.5, Fig. 4.6 and Fig. 4.7. Again, more detailed percent error of the results is shown in Table 4.4. From Fig. 4.8 it is shown that as span-to-camber ratio of bottom chord increases, the horizontal component of cable force in bottom chord obtained by linear solution becomes more and more underestimated, but the difference has a tendency to decrease after l/c gets over 18. The deflection at midspan changes from being somewhat underestimated to being somewhat more overestimated, while the difference of horizontal force in top chord obtained by two solutions remains almost the same.

4.3 Case Study 3: Different Horizontal Pretensions in Chords for a Biconcave Cable Truss

Using the same model as Case Study 1, but this time both the span-to-sag ratio of top chord and the span-to-camber ratio of bottom chord are kept constant at $l/s = l/c = 25$, and the related values are thus given as $d_b = d_t = 0.5$ m and $b_b = b_t = 2.9$ m. Eight different initial horizontal pretension in the bottom chord, H_{0b} = 600, 700, 800, 900, 1000, 1100, 1200, 1300 kN, are considered. The corresponding pretension in the top chord can be estimated using the same formula, $H_{0t} = H_{0b}c/s$, as shown in Case Study 1.

Table 4.5. Analytical results for Case Study 3

| H_{0b}	Nonlinear Solution, 10^3			Linear Solution, 10^3		
	H_b, kN	H_t, kN	w, mm	H_b, kN	H_t, kN	w, mm
600	0.1662	1.515	0.7512	0.0264	1.4825	0.8379
700	0.2758	1.586	0.7282	0.147	1.5508	0.8078
800	0.3864	1.6562	0.7111	0.2662	1.6213	0.7798
900	0.4958	1.7306	0.6901	0.384	1.6938	0.7537
1000	0.6049	1.8052	0.6719	0.5008	1.768	0.7293
1100	0.7137	1.8814	0.6541	0.6164	1.8439	0.7064
1200	0.8221	1.9589	0.6371	0.7312	1.9213	0.6849
1300	0.9302	2.0376	0.6208	0.845	2	0.6646
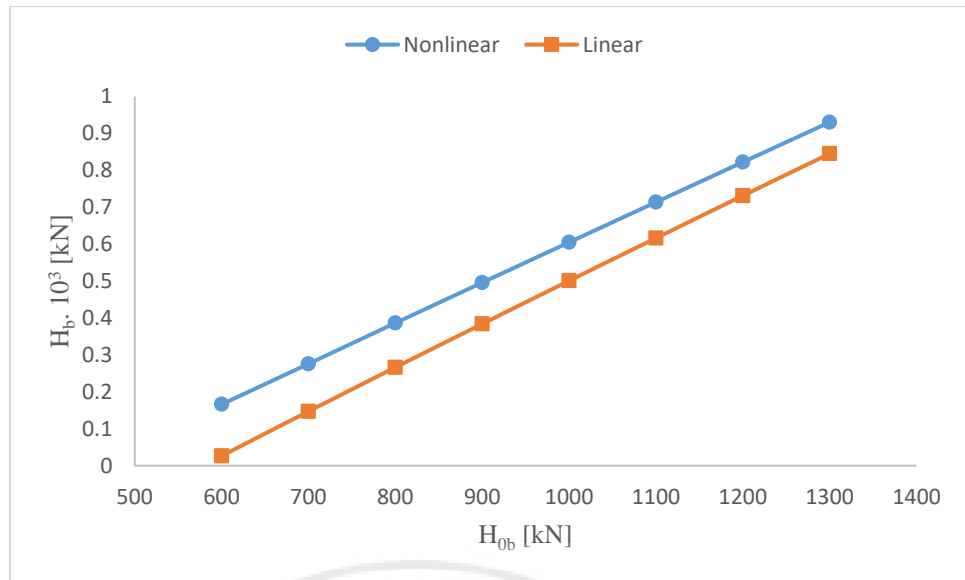
Fig. 4.9. Horizontal force in bottom chord vs. initial horizontal pretension in bottom

chord for a biconcave cable truss
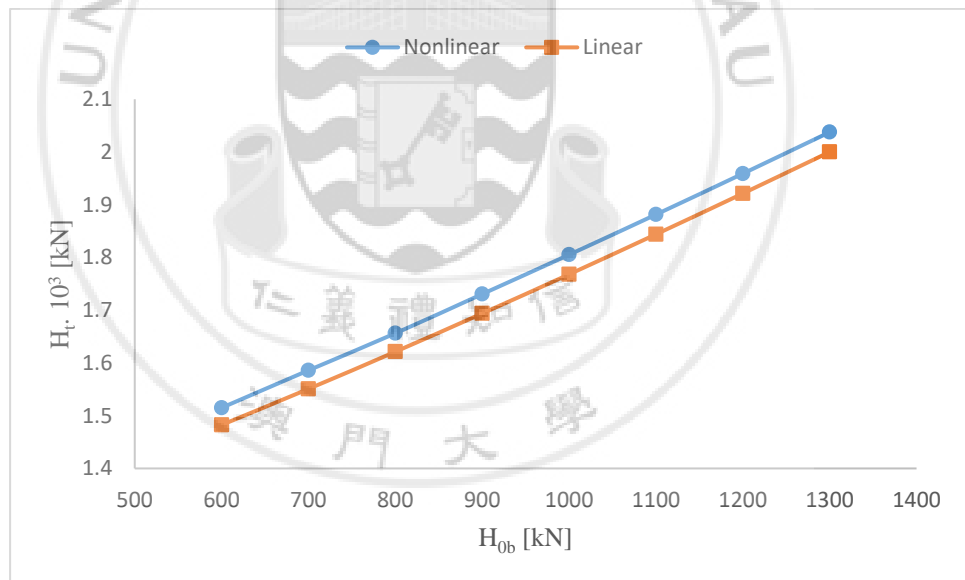
Fig. 4.10. Horizontal force in top chord vs. initial horizontal pretension in bottom
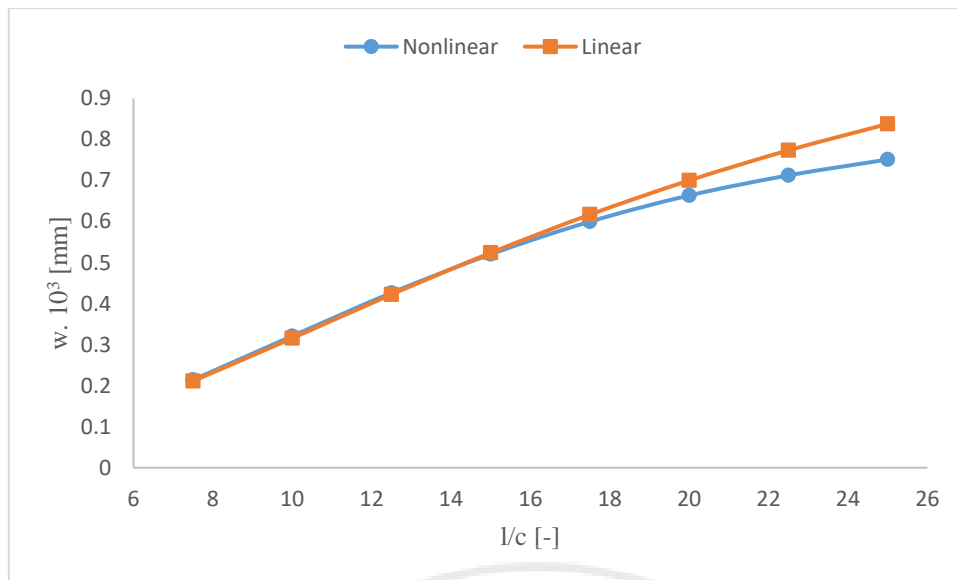
chord for a biconcave cable truss
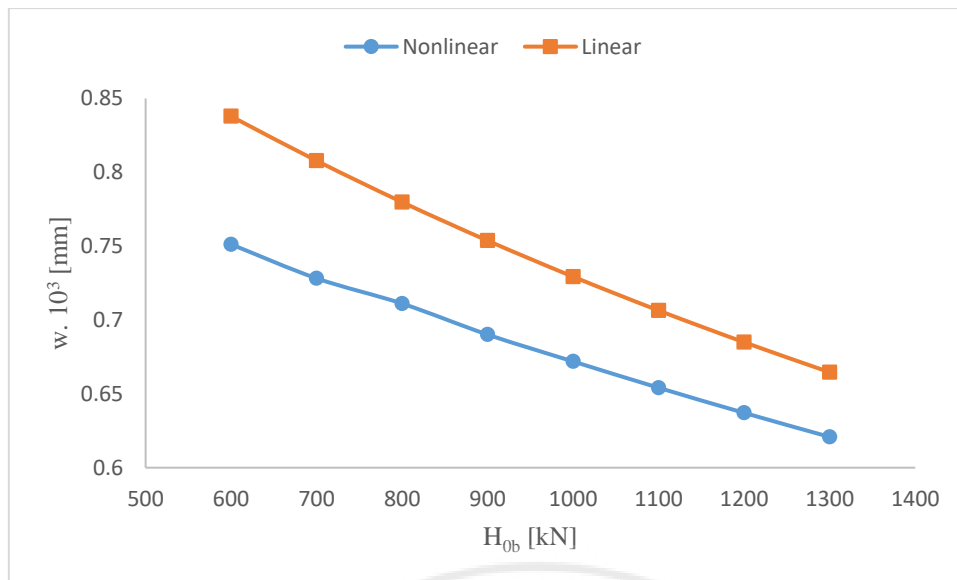
Fig. 4.11. Deflection at midspan vs. initial horizontal pretension in bottom chord for a

biconcave cable truss

Table 4.6. Percent error of results for Case Study 3 (%)

| H_{0b}	600	700	800	900	1000	1100	1200	1300
H_b	84.1	46.7	31.1	22.5	17.2	13.6	11.1	9.2
H_t	2.1	2.2	2.1	2.1	2.1	2.0	1.9	1.8
w	-11.5	-10.9	-9.7	-9.2	-8.5	-8.0	-7.5	-7.1

26
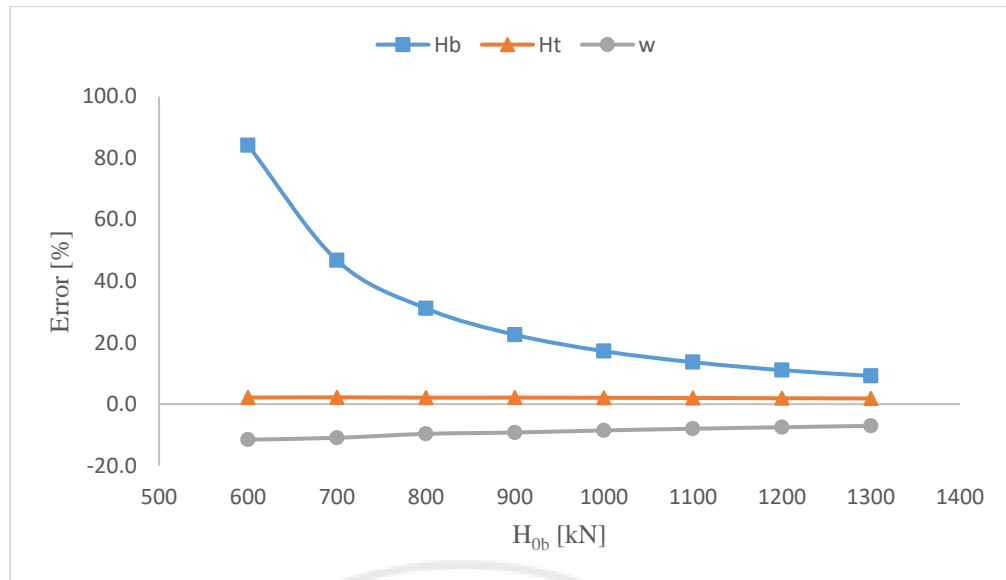
Fig. 4.12. Percent error of results vs. initial horizontal pretension in bottom chord for a biconcave cable truss

Same as Case Study 1, the analytical results in this case are tabulated in Table 4.5 and more straightforward observation can be obtained in Fig. 4.9, Fig. 4.10 and Fig. 4.11. Again, more detailed percent error of the results is shown in Table 4.6. From Fig. 4.12 it is shown that as the initial horizontal component of pretension in bottom chord increases (the corresponding pretension in top chord will also change), the final horizontal force in bottom chord obtained by linear solution becomes less and less underestimated, the overestimation of the deflection at midspan is also somewhat reduced, while the difference of horizontal force in top chord obtained by two solutions remains almost the same.

4.4 Case Study 4: Different Temperature Differences in Top Chord for a Biconcave Cable Truss

Using the same model as Case Study 1, but this time both the span-to-sag ratio of top chord and the span-to-camber ratio of bottom chord are kept constant at $l/s = l/c = 25$, and the related values are thus given as $d_b = d_t = 0.5$ m and $b_b = b_t = 2.9$ m. By assuming the coefficient of expansion of the whole cable truss to be $\alpha = 1.2 \times 10^{-5} / °C$, eight different temperature differences in top chord, ΔT_t = 0, 20, 40, 60, 80, 100, 120 and 140 °C, are considered to take the effect of temperature into account, while no temperature difference occurs in bottom chord.

Table 4.7. Analytical results for Case Study 4

ΔT_t	Nonlinear Solution, 10^3			Linear Solution, 10^3		
	H_b, kN	H_t, kN	w, mm	H_b, kN	H_t, kN	w, mm
0	0.1662	1.515	0.7512	0.0264	1.4825	0.8379
20	0.1819	1.5413	0.7182	0.0483	1.5204	0.8059
40	0.1978	1.5684	0.6854	0.0703	1.5584	0.7738
60	0.2138	1.5963	0.653	0.0922	1.5963	0.7418
80	0.2292	1.6264	0.6179	0.1141	1.6343	0.7097
100	0.2459	1.6557	0.5871	0.1361	1.6722	0.6777
120	0.2626	1.6857	0.5567	0.158	1.7102	0.6457
140	0.2795	1.7163	0.527	0.1799	1.7481	0.6136
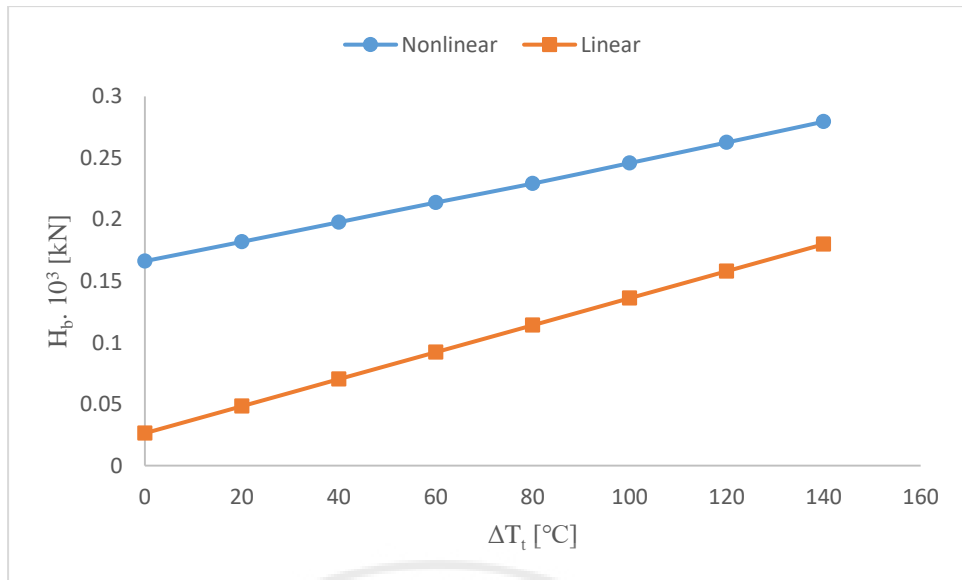
Fig. 4.13. Horizontal force in bottom chord vs. temperature difference in top chord for

a biconcave cable truss

Fig. 4.14. Horizontal force in top chord vs. temperature difference in top chord for a

biconcave cable truss

Fig. 4.15. Deflection at midspan vs. temperature difference in top chord for a
biconcave cable truss

Table 4.8. Percent error of results for Case Study 4 (%)

ΔT_t	0	20	40	60	80	100	120	140
H_b	84.1	73.4	64.5	56.9	50.2	44.7	39.8	35.6
H_t	2.1	1.4	0.6	0.0	-0.5	-1.0	-1.5	-1.9
w	-11.5	-12.2	-12.9	-13.6	-14.9	-15.4	-16.0	-16.4
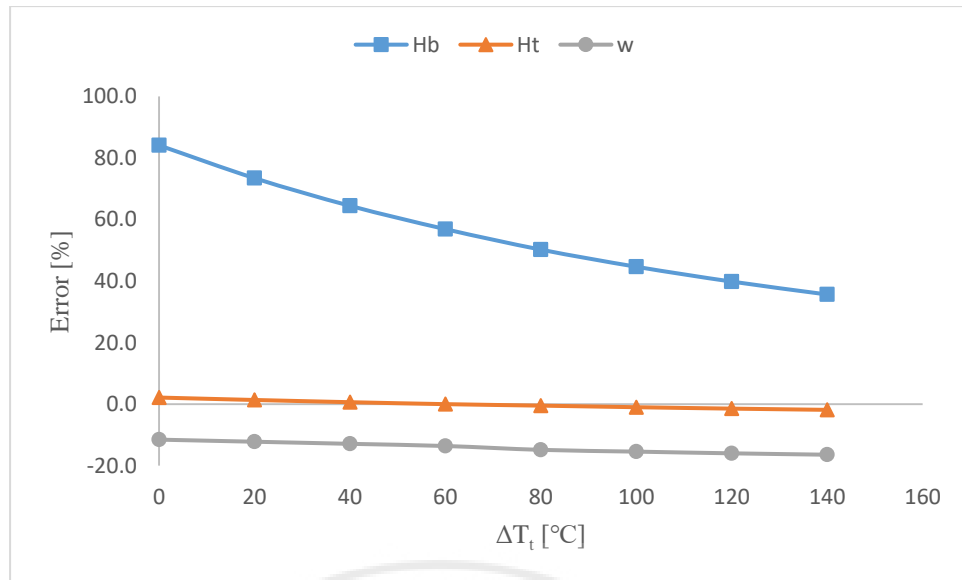
Fig. 4.16. Percent error of results vs. temperature difference in top chord for a biconcave cable truss

Same as Case Study 1, the analytical results in this case are tabulated in Table 4.7 and more straightforward observation can be obtained in Fig. 4.13, Fig. 4.14 and Fig. 4.15. Again, more detailed percent error of the results is shown in Table 4.8. From Fig. 4.16 it is shown that as the temperature difference in top chord increases, the horizontal force in bottom chord obtained by linear solution becomes less and less underestimated, the deflection at midspan becomes slightly more overestimated, while the difference of horizontal force in top chord obtained by two solutions remains almost the same.

4.5 Case Study 5: Different Temperature Differences in Bottom Chord for a Biconcave Cable Truss

Using the same model as Case Study 1, but this time both the span-to-sag ratio of top chord and the span-to-camber ratio of bottom chord are kept constant at $l/s = l/c = 25$, and the related values are thus given as $d_b = d_t = 0.5$ m and $b_b = b_t = 2.9$ m. By assuming the coefficient of expansion of the whole cable truss to be $\alpha = 1.2 \times 10^{-5}/{}^{\circ}\text{C}$, eight different temperature differences in bottom chord, ΔT_b = 0, -20, -40, -60, -80, -100, -120 and -140 ${}^{\circ}\text{C}$, are considered to take the effect of temperature into account, while no temperature difference occurs in top chord. Note that these values are chosen to make sure the analytical results are within the positive range, so that better analysis and comparison can be performed.

Table 4.9. Analytical results for Case Study 5

| ΔT_b	Nonlinear Solution, 10^3			Linear Solution, 10^3		
	H_b, kN	H_t, kN	w, mm	H_b, kN	H_t, kN	w, mm
-140	0.4584	1.617	0.8285	0.2528	1.636	0.9837
-120	0.4164	1.6034	0.8176	0.2205	1.6141	0.9628
-100	0.3744	1.5896	0.8063	0.1881	1.5921	0.942
-80	0.3325	1.5755	0.7949	0.1558	1.5702	0.9212
-60	0.2905	1.5612	0.7831	0.1234	1.5483	0.9004
-40	0.2485	1.5467	0.7711	0.0911	1.5263	0.8795
-20	0.2076	1.5305	0.7624	0.0587	1.5044	0.8587
0	0.1662	1.515	0.7512	0.0264	1.4825	0.8379
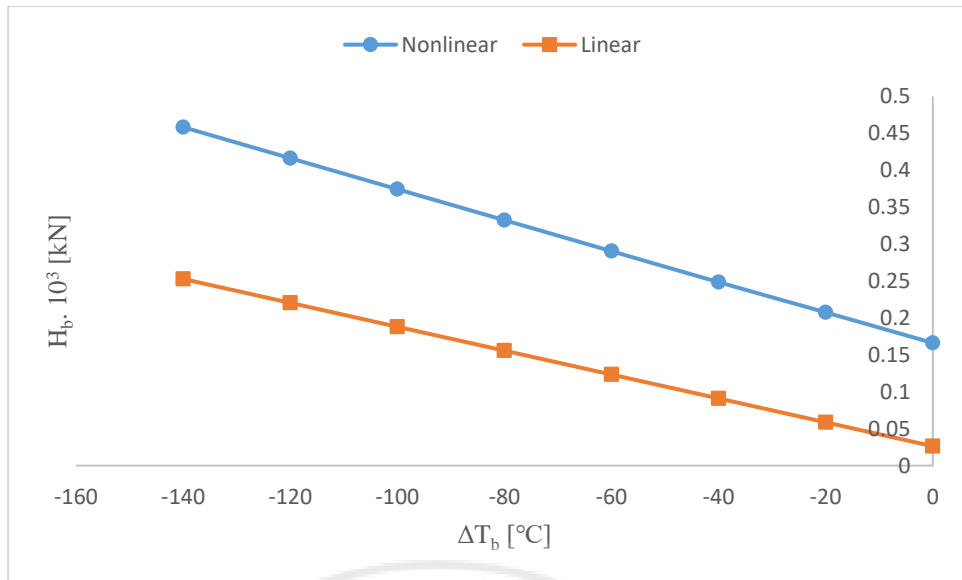
Fig. 4.17. Horizontal force in bottom chord vs. temperature difference in bottom chord
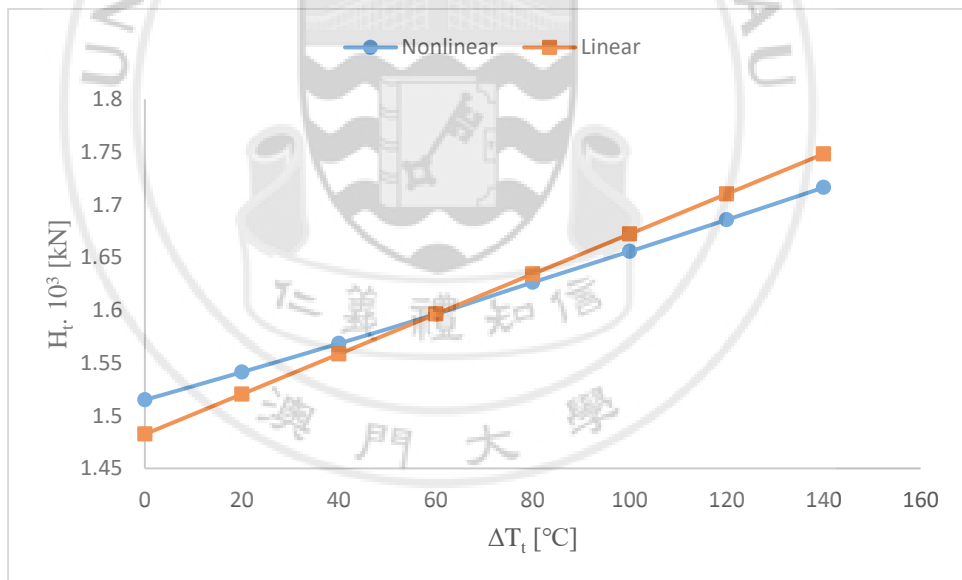
for a biconcave cable truss
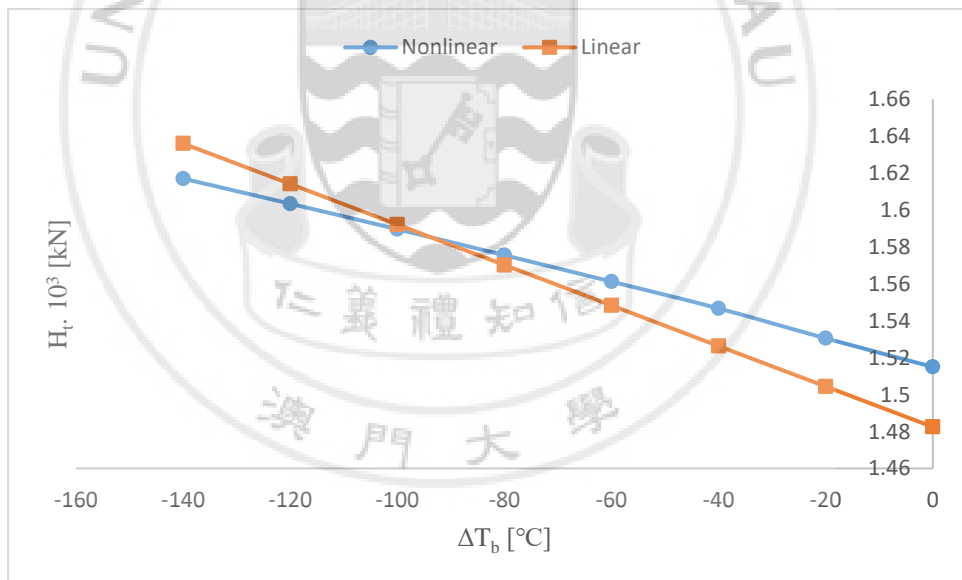
Fig. 4.18. Horizontal force in top chord vs. temperature difference in bottom chord for
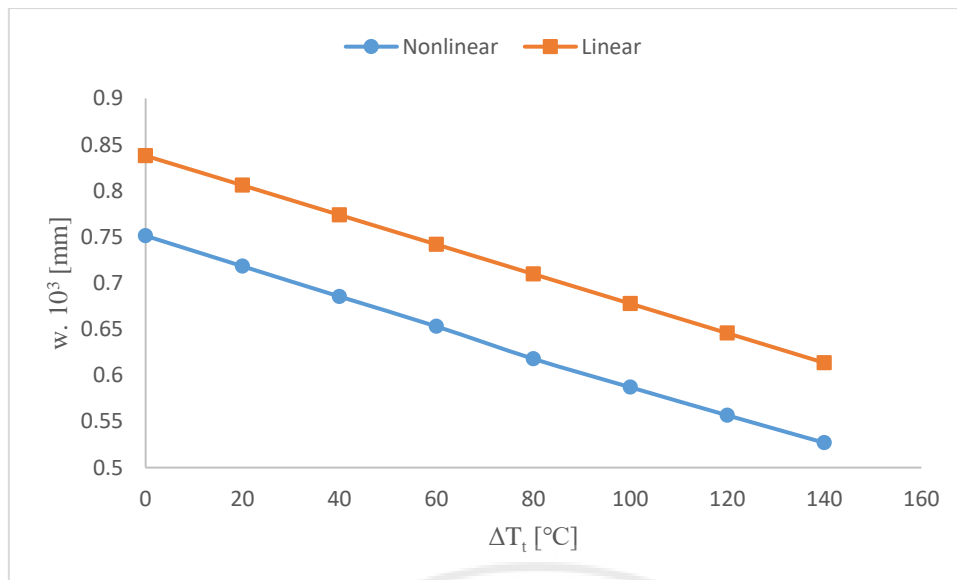
a biconcave cable truss

33

Fig. 4.19. Deflection at midspan vs. temperature difference in bottom chord for a

biconcave cable truss

Table 4.10. Percent error of results for Case Study 5 (%)

| ΔT_b	-140	-120	-100	-80	-60	-40	-20	0
H_b	44.85	47.05	49.76	53.14	57.52	63.34	71.72	84.12
H_t	-1.18	-0.67	-0.16	0.34	0.83	1.32	1.71	2.15
w	-18.73	-17.76	-16.83	-15.89	-14.98	-14.06	-12.63	-11.54
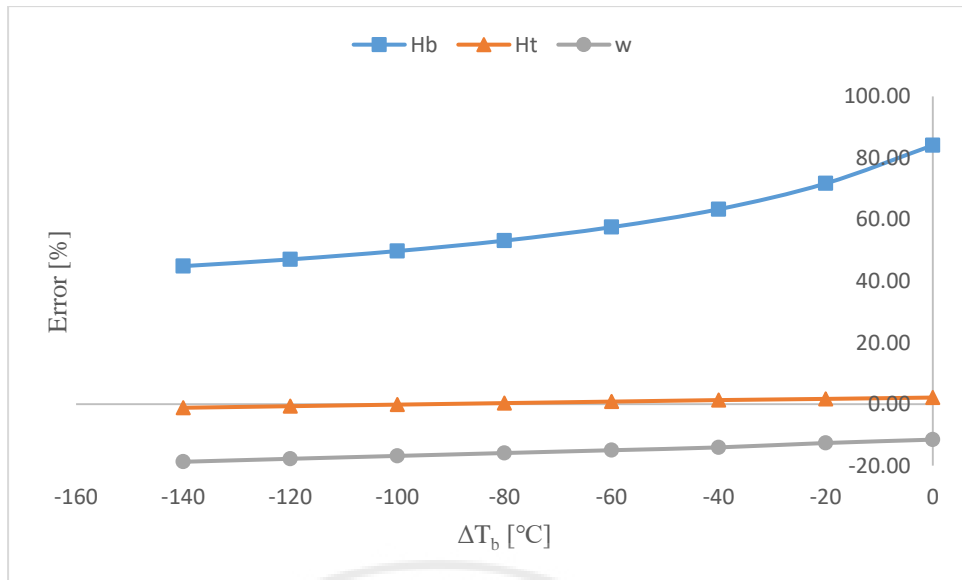
Fig. 4.20. Percent error of results vs. temperature difference in bottom chord for a biconcave cable truss

Same as Case Study 1, the analytical results in this case are tabulated in Table 4.9 and more straightforward observation can be obtained in Fig. 4.17, Fig. 4.18 and Fig. 4.19. Again, more detailed percent error of the results is shown in Table 4.10. From Fig. 4.20 it is shown that as the temperature difference in bottom chord increases, the horizontal force in bottom chord obtained by linear solution becomes more and more underestimated, the deflection at midspan becomes slightly less overestimated, while the difference of horizontal force in top chord obtained by two solutions remains almost the same. It can be seen that the results of changed temperature difference in bottom chord have an overall reverse trend of the ones of changed temperature difference in top chord.

4.6 Case Study 6: Different Span-to-camber Ratios of Top Chord for a Biconvex Cable Truss

Here a biconvex cable truss as shown in Fig. 3.2 is considered (Fig. 3.2 is put here again for convenience and better understanding, but will not be included in the list of figures), of which the span, cross-sectional areas of both bottom and top chords, moduli of elasticity and uniformly distributed load over the entire span are exactly same as the description in Case Study 1.
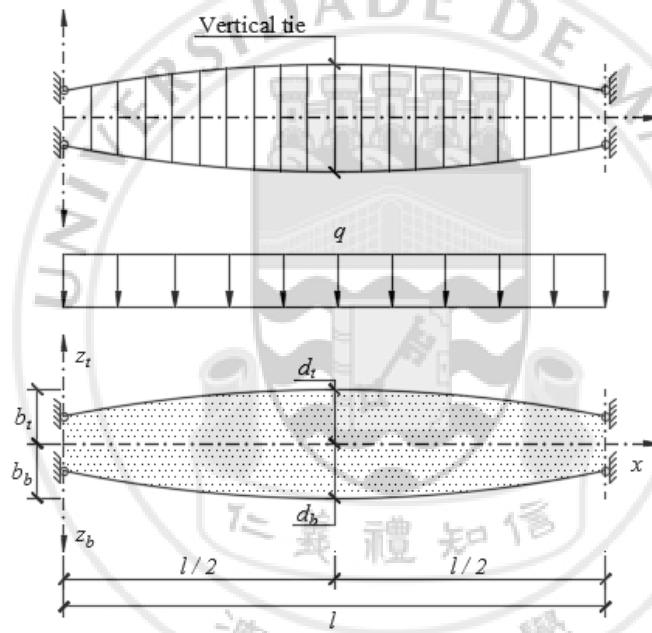
Fig. 3.2. Geometry for biconvex cable truss

This time, eight different span-to-camber ratios of the top chord, $l/c = 7.5$, 10, 12.5, 15, 17.5, 20, 22.5, and 25 are adopted, while the span-to-sag ratio of the bottom chord is kept constant at $l/s = 25$. The other geometrical data are specified as: $b_b = b_t = 0.5$ m, $d_b = 2.9$ m, and $d_t = b_t + c$. The initial horizontal pretention in the bottom chord is

still $H_{0b} = 600.0\,$kN, but the initial horizontal pretention in the top chord should be changed to $H_{0t} = H_{0b}s/c$ due to the changed geometry.

Table 4.11. Analytical results for Case Study 6

l / c	Nonlinear Solution, 10^3			Linear Solution, 10^3		
	H_b, kN	H_t, kN	w, mm	H_b, kN	H_t, kN	w, mm
7.5	0.7193	-0.3387	0.1684	0.7127	-0.3326	0.1647
10	0.795	-0.4148	0.2711	0.7781	-0.4023	0.2601
12.5	0.8883	-0.4585	0.3895	0.8508	-0.4434	0.3663
15	0.9888	-0.4644	0.513	0.9253	-0.4558	0.4752
17.5	1.0862	-0.4319	0.6302	0.9973	-0.4418	0.5803
20	1.1765	-0.3596	0.7312	1.0636	-0.4053	0.6772
22.5	1.2494	-0.2628	0.8115	1.1226	-0.3508	0.7634
25	1.3049	-0.1512	0.8715	1.1736	-0.2825	0.8379
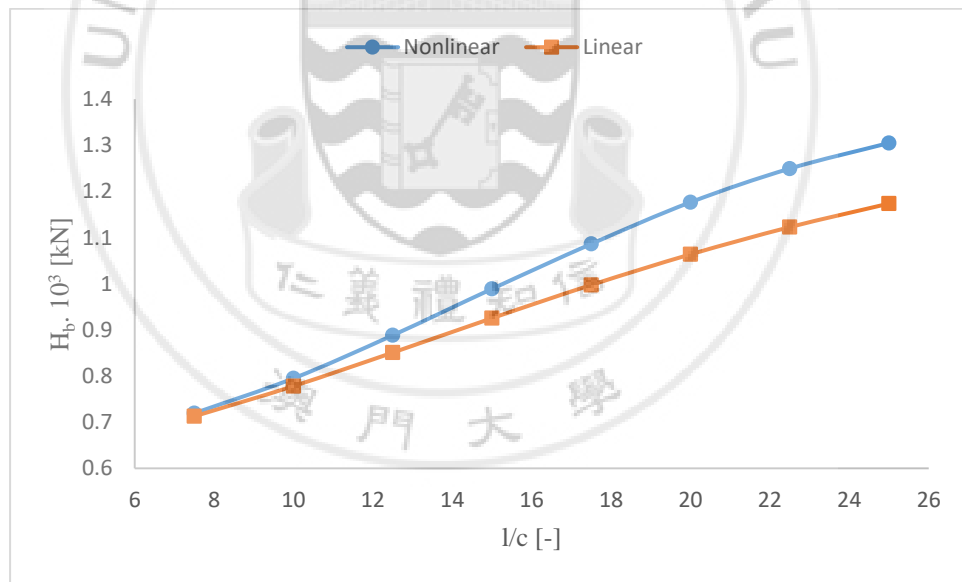
Fig. 4.21. Horizontal force in bottom chord vs. span-to-camber ratio in top chord for a biconvex cable truss

Fig. 4.22. Horizontal force in top chord vs. span-to-camber ratio in top chord for a
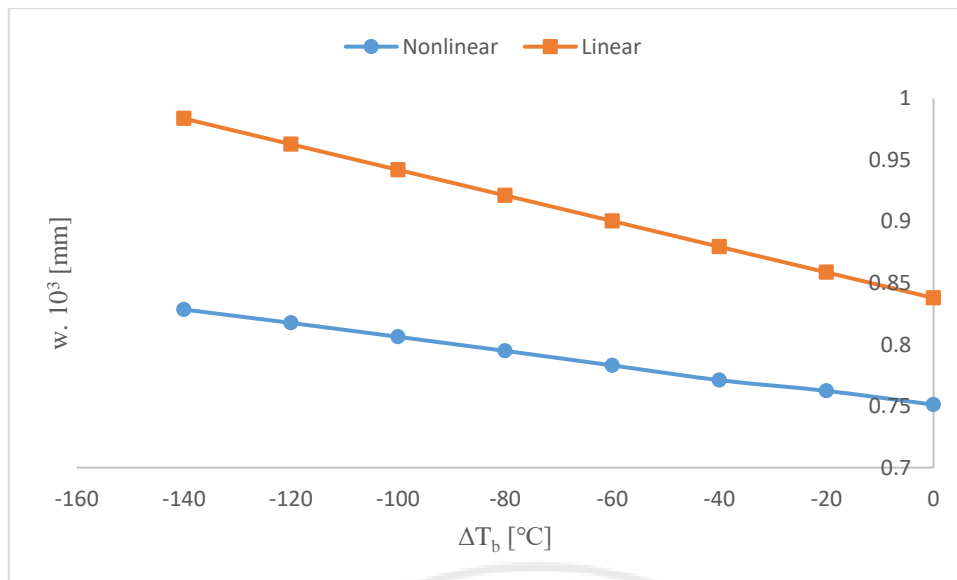
biconvex cable truss

Fig. 4.23. Deflection at midspan vs. span-to-camber ratio in top chord for a biconvex

cable truss

Table 4.12. Percent error of results for Case Study 6 (%)

l / c	7.5	10	12.5	15	17.5	20	22.5	25
H_b	0.92	2.13	4.22	6.42	8.18	9.60	10.15	10.06
H_t	1.80	3.01	3.29	1.85	-2.29	-12.71	-33.49	-86.84
w	2.20	4.06	5.96	7.37	7.92	7.39	5.93	3.86
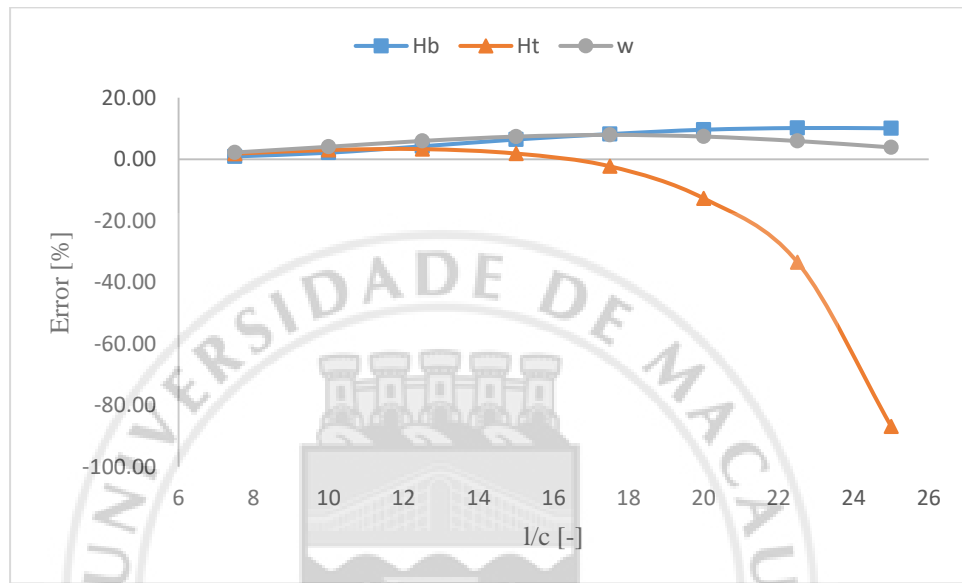
Fig. 4.24. Percent error of results vs. span-to-camber ratio in top chord for a biconvex

cable truss

Same as Case Study 1, the analytical results in this case are tabulated in Table 4.11 and more straightforward observation can be obtained in Fig. 4.21, Fig. 4.22 and Fig. 4.23. The negative values shown in the table and graph for horizontal force in top chord indicate that, for a biconvex cable truss even with pretension in chords, the top chord is mainly carrying compression. Again, more detailed percent error of the results is shown in Table 4.12. From Fig. 4.24 it is shown that as the span-to-camber ratio in top chord increases, the horizontal force in bottom chord obtained by linear solution gets slightly more underestimated, but the underestimation has a trend to decrease when the ratio increases to a particular value. The difference of deflection at midspan obtained by two

solutions remains almost the same. The horizontal force in top chord changes from being somewhat underestimated to being quite more overestimated.

4.7 Case Study 7: Different Span-to-sag Ratios of Bottom Chord for a Biconvex Cable Truss

Using the same model as Case Study 6, but this time eight different span-to-sag ratios of the bottom chord, l/s = 7.5, 10, 12.5, 15, 17.5, 20, 22.5, and 25 are adopted, while the span-to-camber ratio of the top chord is kept constant at l/c = 25. The other geometrical data are specified as: $b_b = b_t = 0.5$ m, $d_b = b_b + s$ and $d_t = b_t + c$.

Table 4.13. Analytical results for Case Study 7

| l/s	Nonlinear Solution, 10^3			Linear Solution, 10^3		
	H_b, kN	H_t, kN	w, mm	H_b, kN	H_t, kN	w, mm
7.5	1.0264	1.7904	0.208	1.0272	1.7776	0.2111
10	1.1093	1.1952	0.3093	1.1066	1.1676	0.3156
12.5	1.1688	0.8021	0.4134	1.1569	0.7554	0.4222
15	1.2119	0.5156	0.5152	1.1845	0.4483	0.5238
17.5	1.2439	0.2945	0.6124	1.1955	0.2074	0.6169
20	1.2685	0.1172	0.7041	1.1949	0.0126	0.7002
22.5	1.2883	-0.0287	0.7905	1.1867	-0.1481	0.7736
25	1.3049	-0.1512	0.8715	1.1736	-0.2825	0.8379
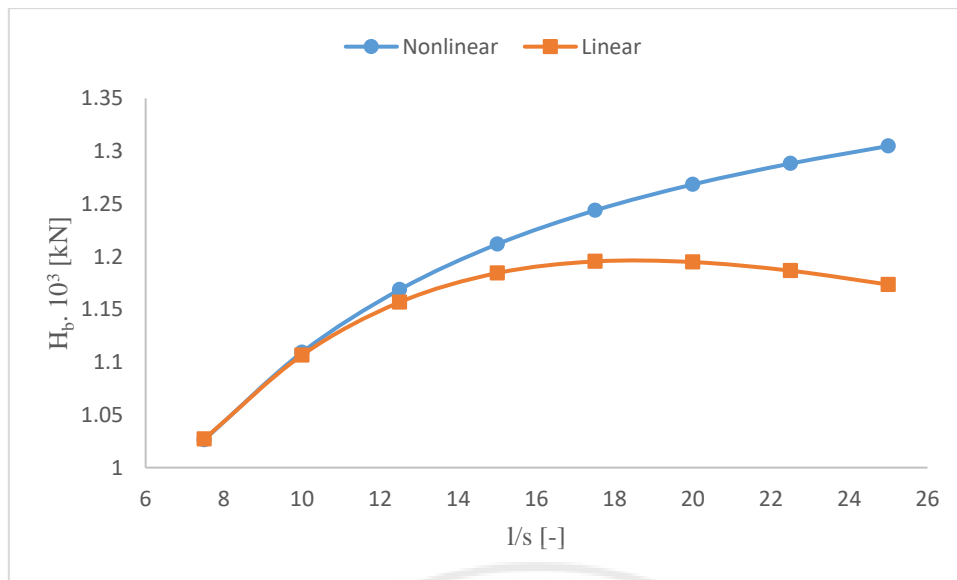
Fig. 4.25. Horizontal force in bottom chord vs. span-to-sag ratio in bottom chord for a
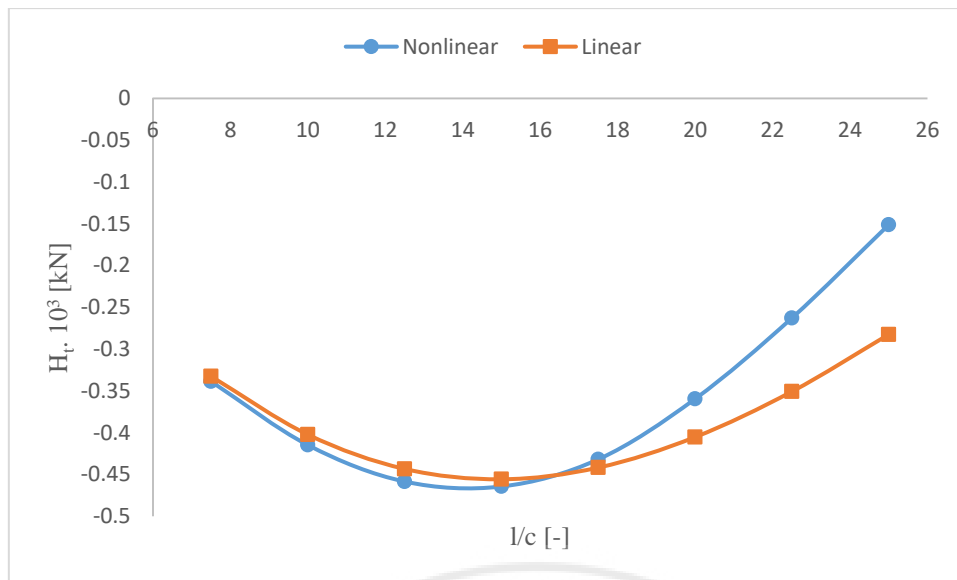
biconvex cable truss
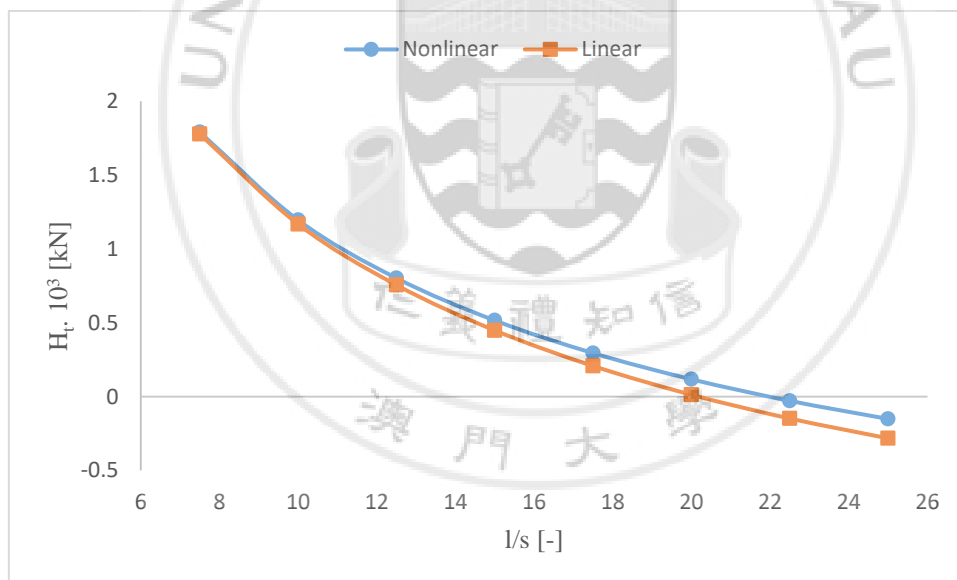
Fig. 4.26. Horizontal force in top chord vs. span-to-sag ratio in bottom chord for a
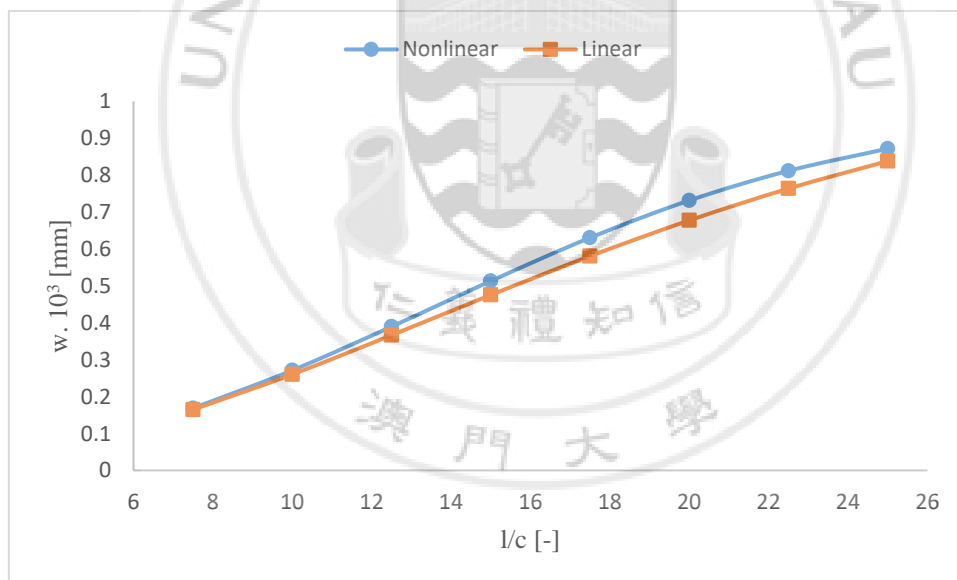
biconvex cable truss

42

Fig. 4.27. Deflection at midspan vs. span-to-sag ratio in bottom chord for a biconvex

cable truss

Table 4.14. Percent error of results for Case Study 7 (%)

| l / s	7.5	10	12.5	15	17.5	20	22.5	25
H_b	-0.08	0.24	1.02	2.26	3.89	5.80	7.89	10.06
H_t	0.71	2.31	5.82	13.05	29.58	89.25	-416.0	-86.84
w	-1.49	-2.04	-2.13	-1.67	-0.73	0.55	2.14	3.86
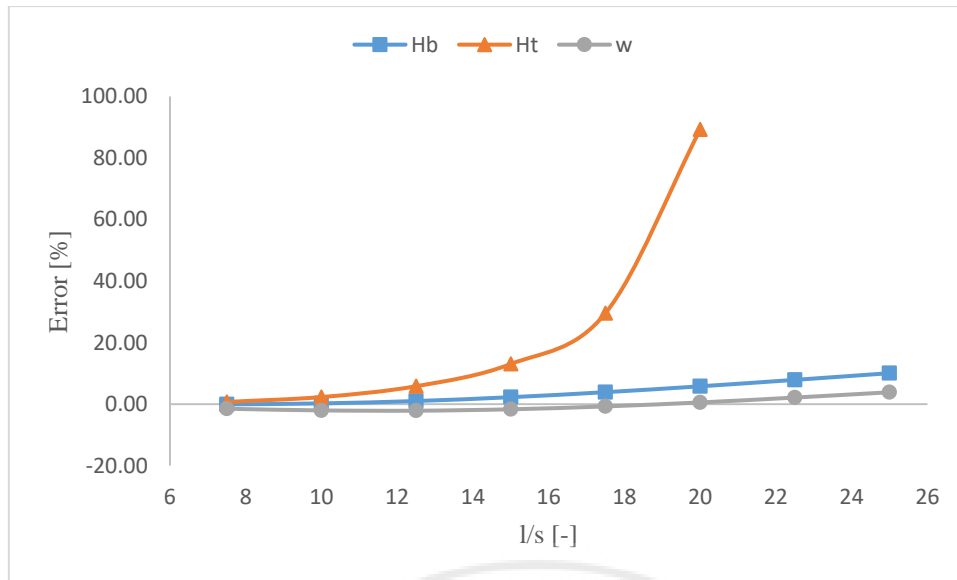
Fig. 4.28. Percent error of results vs. span-to-sag ratio in bottom chord for a biconvex cable truss

Same as Case Study 1, the analytical results in this case are tabulated in Table 4.13 and more straightforward observation can be obtained in Fig. 4.25, Fig. 4.26 and Fig. 4.27. The negative values shown in the table and graph for horizontal force in top chord indicate the chord is carrying compression. Again, more detailed percent error of the results is shown in Table 4.14. However, for the corresponding graph plot, the values adopted for horizontal force in top chord are those within tension range only, so as to make the analysis consistent and meaningful. From Fig. 4.28 it is shown that as the span-to-sag ratio in bottom chord increases, the horizontal force in bottom chord obtained by linear solution gets slightly more underestimated, the horizontal force in top chord becomes quite more underestimated, while the difference of deflection at midspan obtained by two solutions remains almost the same.

4.8 Case Study 8: Different Horizontal Pretensions in Chords for a Biconvex Cable Truss

Using the same model as Case Study 6, but this time both the span-to-camber ratio of top chord and the span-to-sag ratio of bottom chord are kept constant at $l/c = l/s = 25$, and the related values are thus given as $b_b = b_t = 0.5$ m and $d_b = d_t = 2.9$ m. Eight different initial horizontal pretension in the bottom chord, $H_{0b} = $ 900, 1000, 1100, 1200, 1300, 1400, 1500 and 1600 kN, are considered. The corresponding pretension in the top chord can be estimated using the same formula, $H_{0t} = H_{0b}s/c$, as shown in Case Study 6. Note that these values are chosen so that both the nonlinear and linear solution are within the tension range, which makes the analysis more consistent and meaningful.

Table 4.15. Analytical results for Case Study 8

| H_{0b}	Nonlinear Solution, 10^3			Linear Solution, 10^3		
	H_b, kN	H_t, kN	w, mm	H_b, kN	H_t, kN	w, mm
900	1.5218	0.2111	0.7815	1.416	0.1062	0.7537
1000	1.5978	0.33	0.7559	1.4992	0.232	0.7293
1100	1.6759	0.4475	0.7309	1.5836	0.3561	0.7064
1200	1.7556	0.5641	0.7071	1.6688	0.4787	0.6849
1300	1.8367	0.6801	0.6851	1.755	0.6	0.6646
1400	1.9187	0.7959	0.665	1.8419	0.7201	0.6456
1500	2.0019	0.9108	0.6459	1.9296	0.8391	0.6276
1600	2.0861	1.025	0.6278	2.018	0.957	0.6105
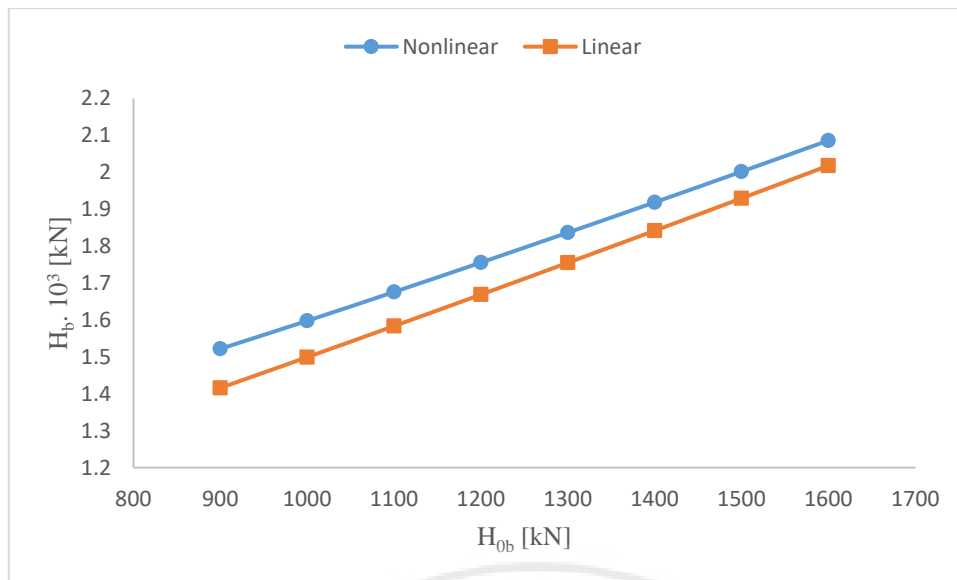
Fig. 4.29. Horizontal force in bottom chord vs. initial horizontal pretension in bottom

chord for a biconvex cable truss
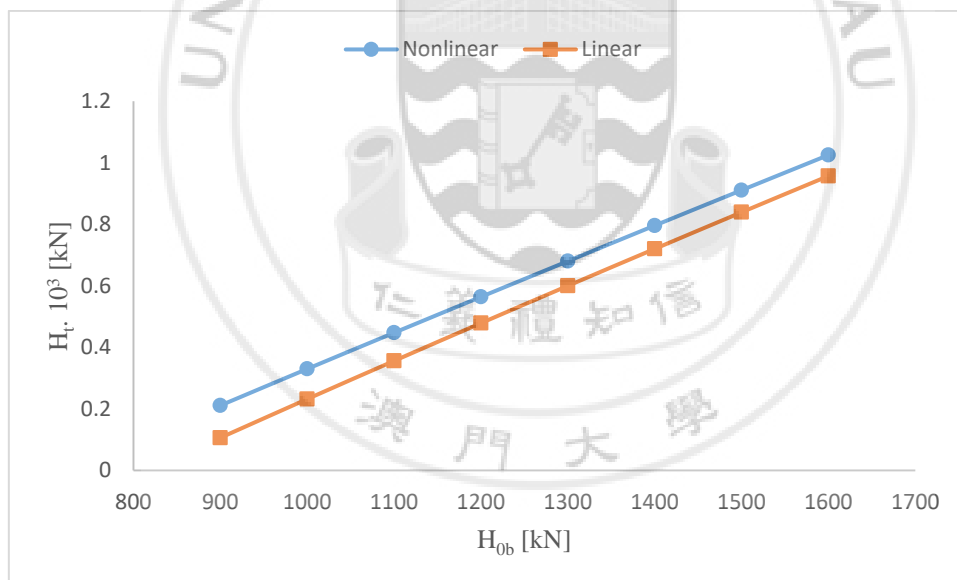
Fig. 4.30. Horizontal force in top chord vs. initial horizontal pretension in bottom
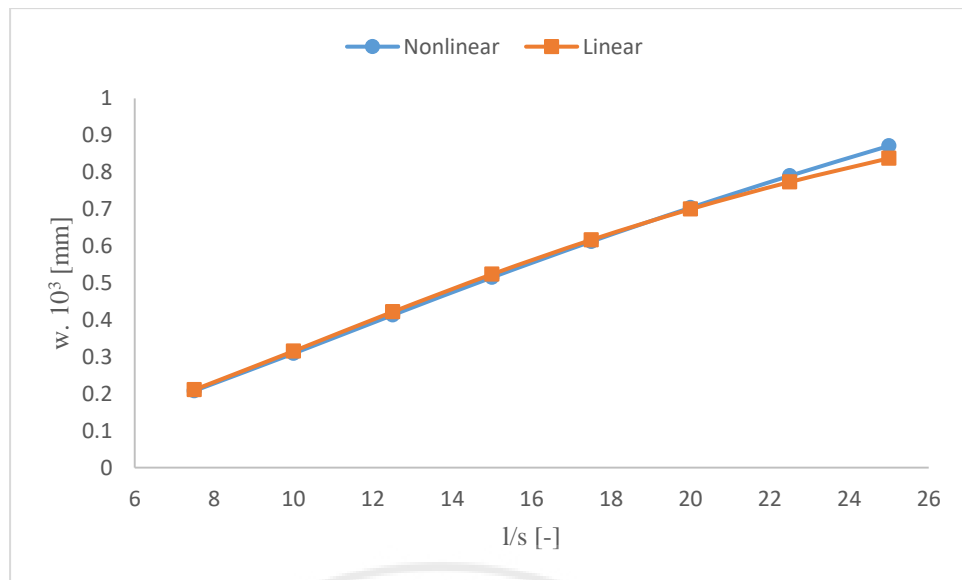
chord for a biconvex cable truss
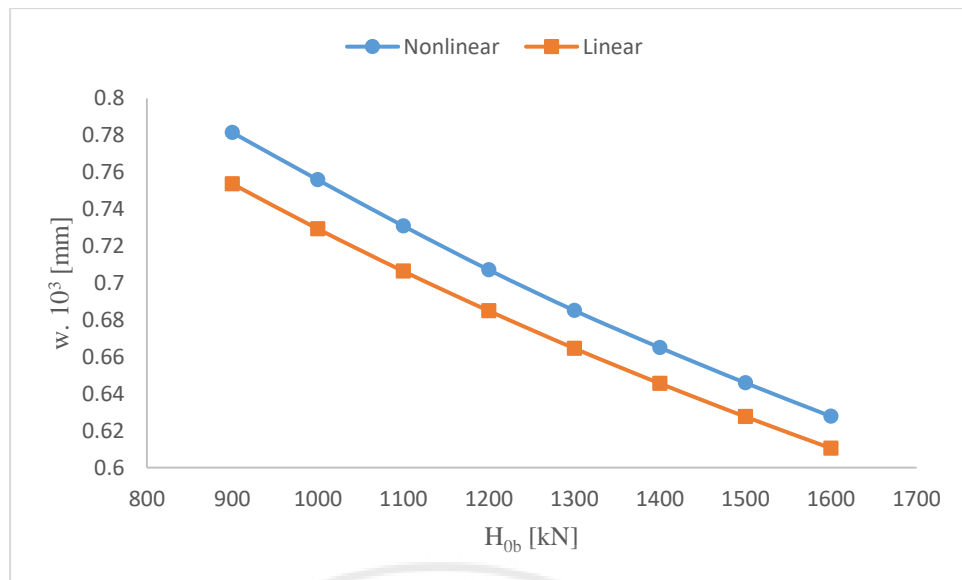
Fig. 4.31. Deflection at midspan vs. initial horizontal pretension in bottom chord for a

biconvex cable truss

Table 4.16. Percent error of results for Case Study 8 (%)

H_{0b}	900	1000	1100	1200	1300	1400	1500	1600
H_b	6.95	6.17	5.51	4.94	4.45	4.00	3.61	3.26
H_t	49.69	29.70	20.42	15.14	11.78	9.52	7.87	6.63
w	3.56	3.52	3.35	3.14	2.99	2.92	2.83	2.76
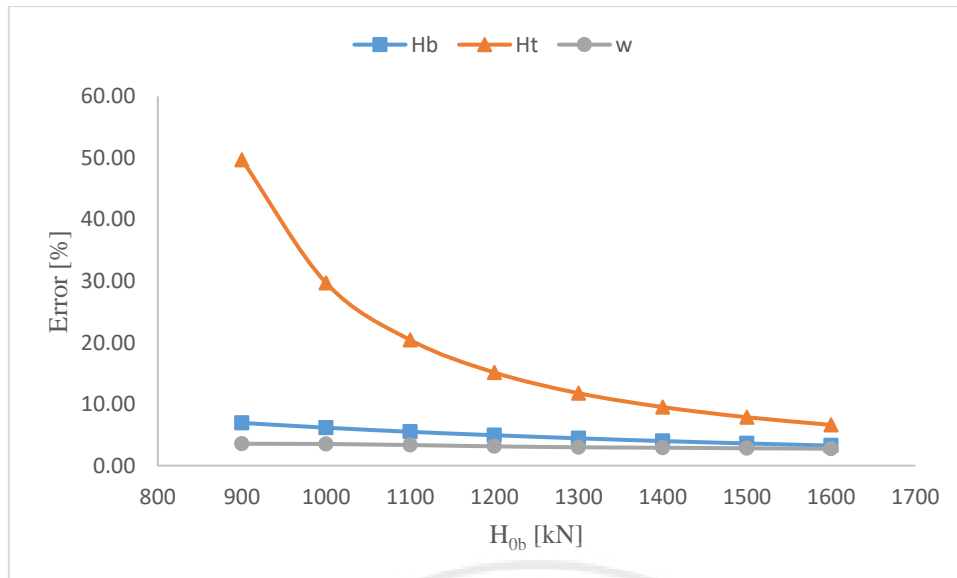
Fig. 4.32. Percent error of results vs. initial horizontal pretension in bottom chord for a biconvex cable truss

Same as Case Study 1, the analytical results in this case are tabulated in Table 4.15 and more straightforward observation can be obtained in Fig. 4.29, Fig. 4.30 and Fig. 4.31. Again, more detailed percent error of the results is shown in Table 4.16. From Fig. 4.32 it is shown that as the initial horizontal pretension in bottom chord increases, the horizontal force in bottom chord obtained by linear solution gets slightly less underestimated, the underestimation of horizontal force in top chord reduces even more, while the difference of deflection at midspan obtained by two solutions remains almost the same.

4.9 Case Study 9: Different Temperature Differences in Top Chord for a Biconvex Cable Truss

Using the same model as Case Study 6, but this time both the span-to-camber ratio of top chord and the span-to-sag ratio of bottom chord are kept constant at $l/c = l/s = 25$, and the related values are thus given as $b_b = b_t = 0.5$ m and $d_b = d_t = 2.9$ m. By assuming the coefficient of expansion of the whole cable truss to be $\alpha = 1.2 \times 10^{-5}/℃$, eight different temperature differences in top chord, $\Delta T_t =$ 0, -20, -40, -60, -80, -100, -120 and -140 ℃, are considered to take the effect of temperature into account, while no temperature difference occurs in bottom chord. Note that these values are chosen so that both the nonlinear and linear solutions lies on pure tension or compression range, which makes the analysis more consistent and meaningful.

Table 4.17. Analytical results for Case Study 9

ΔT_t	Nonlinear Solution, 10^3			Linear Solution, 10^3		
	H_b, kN	H_t, kN	w, mm	H_b, kN	H_t, kN	w, mm
-140	1.155	-0.5381	0.7076	1.0201	-0.5481	0.6136
-120	1.1784	-0.4847	0.7332	1.042	-0.5102	0.6457
-100	1.2009	-0.4309	0.7581	1.0639	-0.4722	0.6777
-80	1.2228	-0.3764	0.7822	1.0859	-0.4343	0.7097
-60	1.2441	-0.3211	0.8056	1.1078	-0.3963	0.7418
-40	1.2648	-0.2652	0.8283	1.1297	-0.3584	0.7738
-20	1.2851	-0.2085	0.8502	1.1517	-0.3204	0.8059
0	1.3049	-0.1512	0.8715	1.1736	-0.2825	0.8379
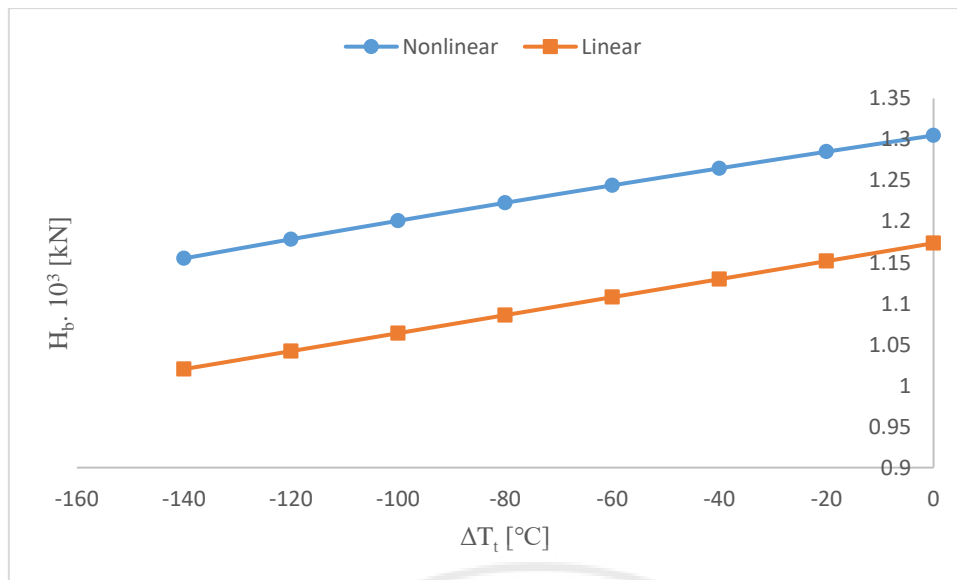
Fig. 4.33. Horizontal force in bottom chord vs. temperature difference in top chord for

a biconvex cable truss

Fig. 4.34. Horizontal force in top chord vs. temperature difference in top chord for a

biconvex cable truss

Fig. 4.35. Deflection at midspan vs. temperature difference in top chord for a

biconvex cable truss

Table 4.18. Percent error of results for Case Study 9 (%)

ΔT_t	-140	-120	-100	-80	-60	-40	-20	0
H_b	11.68	11.58	11.41	11.20	10.96	10.68	10.38	10.06
H_t	-1.86	-5.26	-9.58	-15.38	-23.42	-35.14	-53.67	-86.84
w	13.28	11.93	10.61	9.27	7.92	6.58	5.21	3.86
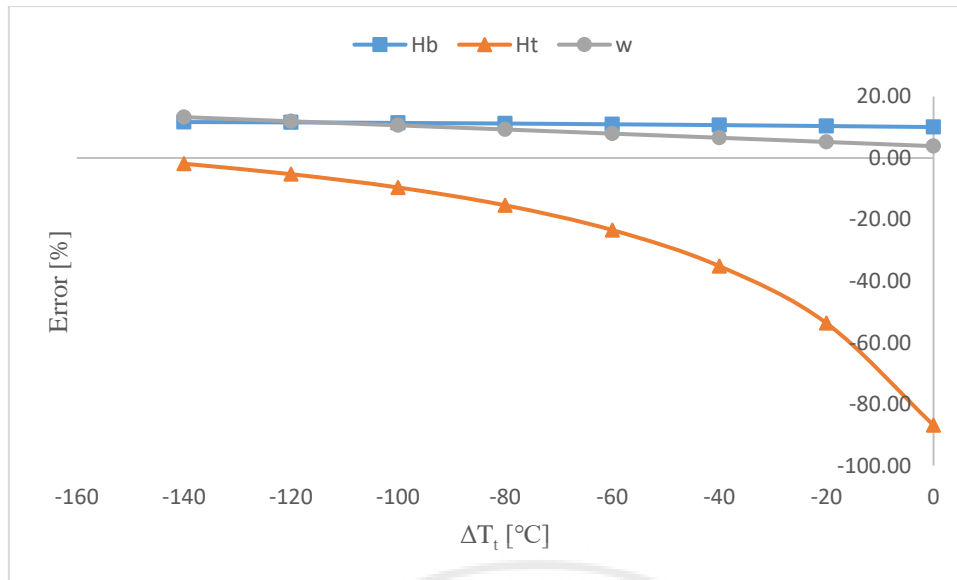
Fig. 4.36. Percent error of results vs. temperature difference in top chord for a biconvex cable truss

Same as Case Study 1, the analytical results in this case are tabulated in Table 4.17 and more straightforward observation can be obtained in Fig. 4.33, Fig. 4.34 and Fig. 4.35. Again, more detailed percent error of the results is shown in Table 4.18. From Fig. 4.36 it is shown that as the temperature difference in top chord increases, the deflection at midspan obtained by linear solution gets slightly less underestimated, the horizontal force in top chord becomes more and more overestimated in terms of compression, while the difference of horizontal force in bottom chord obtained by two solutions remains almost the same.

4.10 Case Study 10: Different Temperature Differences in Bottom Chord for a Biconvex Cable Truss

Using the same model as Case Study 6, but this time both the span-to-camber ratio of top chord and the span-to-sag ratio of bottom chord are kept constant at $l/c = l/s = 25$, and the related values are thus given as $b_b = b_t = 0.5$ m and $d_b = d_t = 2.9$ m. By assuming the coefficient of expansion of the whole cable truss to be $\alpha = 1.2 \times 10^{-5}/°C$, eight different temperature differences in bottom chord, ΔT_b = 0, 20, 40, 60, 80, 100, 120 and 140 °C, are considered to take the effect of temperature into account, while no temperature difference occurs in top chord. Note that these values are chosen so that both the nonlinear and linear solutions lies on pure tension or compression range, which makes the analysis more consistent and meaningful.

Table 4.19. Analytical results for Case Study 10

| ΔT_b	Nonlinear Solution, 10^3			Linear Solution, 10^3		
	H_b, kN	H_t, kN	w, mm	H_b, kN	H_t, kN	w, mm
0	1.3049	-0.1512	0.8715	1.1736	-0.2825	0.8379
20	1.2858	-0.1707	0.9008	1.1413	-0.3044	0.8587
40	1.2673	-0.1901	0.9306	1.1089	-0.3263	0.8795
60	1.2494	-0.2093	0.9607	1.0766	-0.3483	0.9004
80	1.2321	-0.2284	0.9911	1.0442	-0.3702	0.9212
100	1.2155	-0.2472	1.022	1.0119	-0.3921	0.942
120	1.1994	-0.266	1.0532	0.9795	-0.4141	0.9628
140	1.184	-0.2844	1.0847	0.9472	-0.436	0.9837
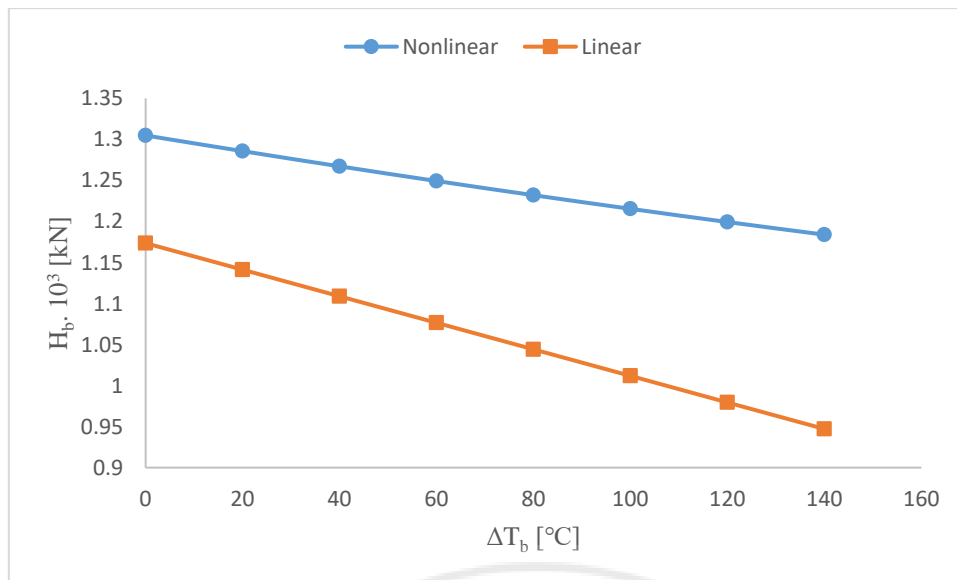
Fig. 4.37. Horizontal force in bottom chord vs. temperature difference in bottom chord

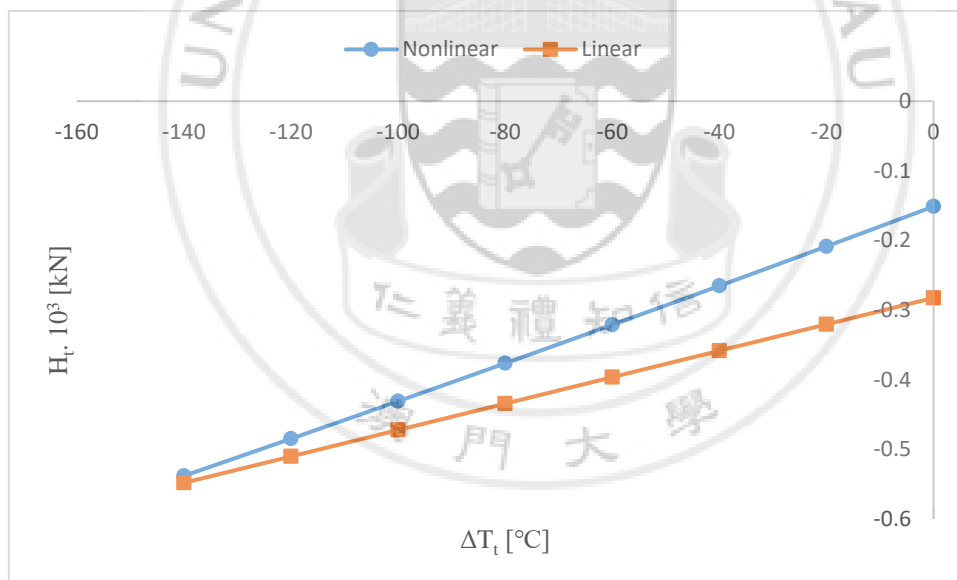for a biconvex cable truss
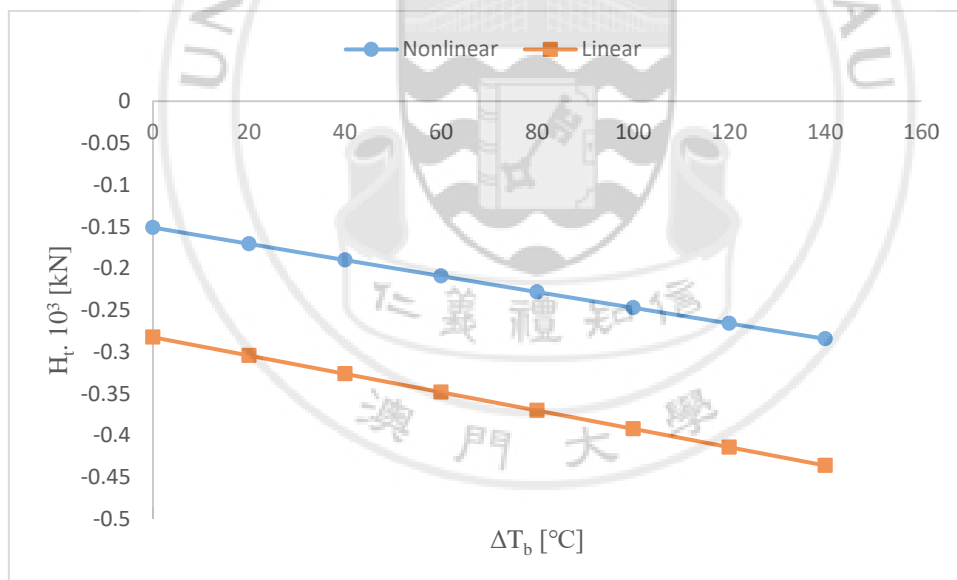
Fig. 4.38. Horizontal force in top chord vs. temperature difference in bottom chord for
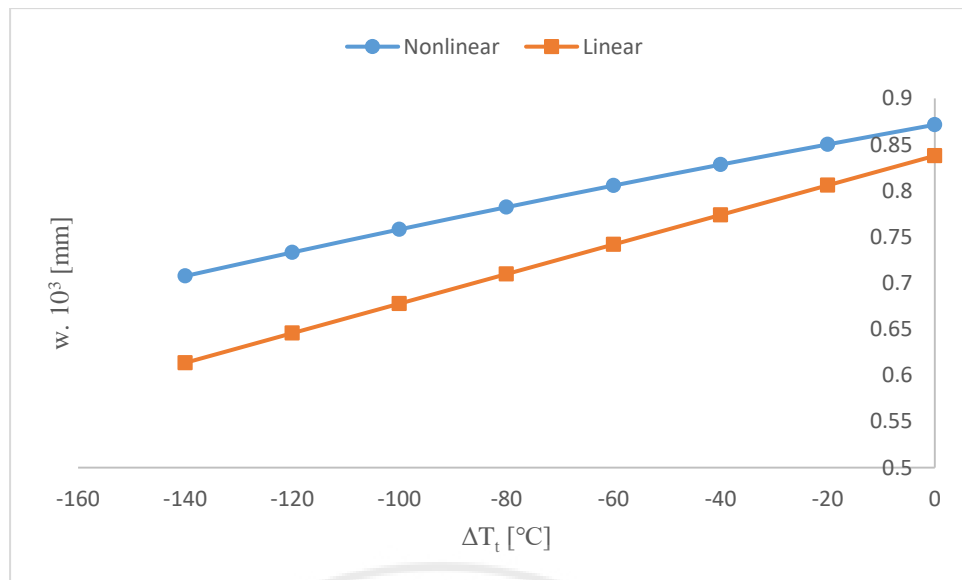
a biconvex cable truss
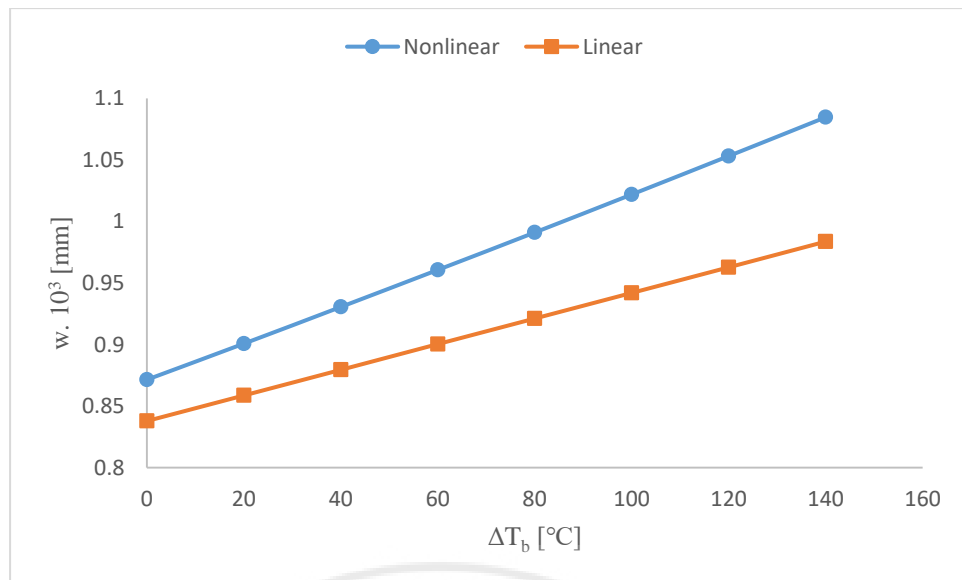
Fig. 4.39. Deflection at midspan vs. temperature difference in bottom chord for a

biconvex cable truss

Table 4.20. Percent error of results for Case Study 10 (%)

ΔT_b	0	20	40	60	80	100	120	140
H_b	10.06	11.24	12.50	13.83	15.25	16.75	18.33	20.00
H_t	-86.84	-78.32	-71.65	-66.41	-62.08	-58.62	-55.68	-53.31
w	3.86	4.67	5.49	6.28	7.05	7.83	8.58	9.31
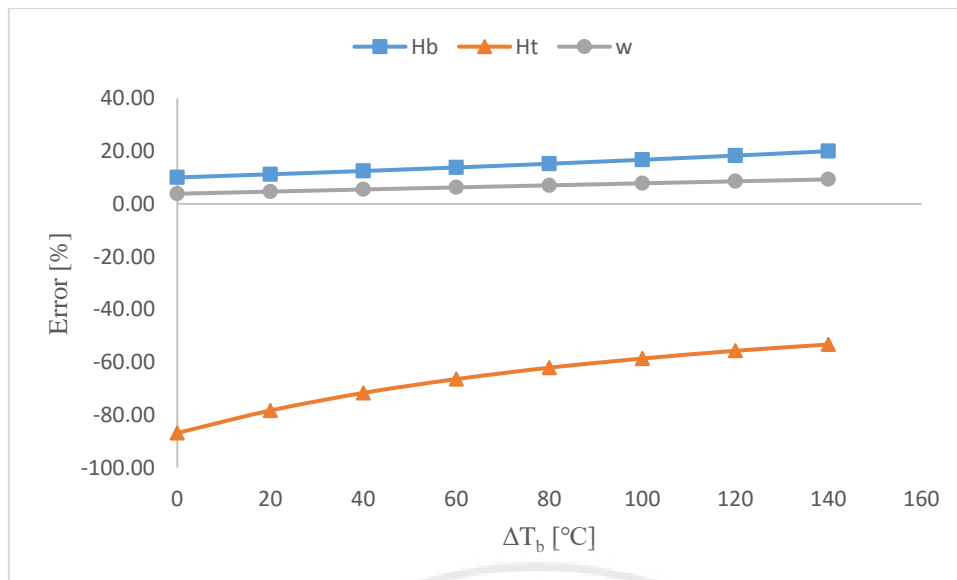
Fig. 4.40. Percent error of results vs. temperature difference in bottom chord for a biconvex cable truss

Same as Case Study 1, the analytical results in this case are tabulated in Table 4.19 and more straightforward observation can be obtained in Fig. 4.37, Fig. 4.38 and Fig. 4.39. Again, more detailed percent error of the results is shown in Table 4.20. From Fig. 4.40 it is shown that as the temperature difference in bottom chord increases, the horizontal force in bottom chord obtained by linear solution gets slightly more underestimated, the horizontal force in top chord becomes less overestimated in terms of compression, while the difference of deflection at midspan obtained by two solutions remains almost the same.

CHAPTER 5 CONCLUSION AND RECOMMENDATIONS

In this thesis, the nonlinear and linear solutions for cable trusses are derived following the procedures proposed by Irvine (1981) with the self-weight of cables ignored. After the solutions are obtained, 10 cases are assumed with different parameter values changed to study the effect each parameter will have on the difference of results from nonlinear and linear approaches. By developing a program of *MATLAB 2016b*, the corresponding closed-form equations are solved and the results are tabulated in tables and plotted in figures for better analysis.

The parameters l/s, l/c, H_{0b}, ΔT_t and ΔT_b in a biconcave cable truss are studied from section 4.1 to section 4.5, while same parameters in a biconvex cable truss are studied from section 4.6 to section 4.10. In this chapter, the results obtained in chapter 4 will be reorganized to provide a better idea how the resultant horizontal forces in bottom and top chords and the deflection at midspan are affected by the parameters mentioned above. However, it should be noted that all the conclusions made here are within a limited range. Since it is not practical to extend the value of interest to infinity, only some relatively typical ones are chosen. Also, these changing values in each case are assumed in a way that most of the corresponding results are within pure positive or negative range, which can make the analysis more consistent and meaningful in a manner. All the following conclusions are based on this kind of assumed ranges, and this should be noted throughout this chapter. For the results out of this range, to some degree, predictions can be made according to the existing data shown in this thesis.

5.1 Biconcave Cable Truss

For the resultant horizontal force in bottom chord, H_b, obtained by linear solution, compared with the one obtained by nonlinear solution:

(1) As the span-to-sag ratio of top chord increases, it becomes quite more underestimated.

(2) As the span-to-camber ratio of bottom chord increases, it becomes quite more underestimated at first, and gets slightly less underestimated afterwards.

(3) As the pretension in chords increases, it becomes quite less underestimated.

(4) As the temperature difference in top chord increases from 0, it becomes quite less underestimated.

(5) As the temperature difference in bottom chord increases from negative value to 0, it becomes more underestimated to some degree.

For the resultant horizontal force in top chord, H_t, obtained by linear solution, compared with the one obtained by nonlinear solution:

(1) As the span-to-sag ratio of top chord increases, the difference remains almost the same.

(2) As the span-to-camber ratio of bottom chord increases, the difference remains almost the same.

(3) As the pretension in chords increases, the difference remains almost the same.

(4) As the temperature difference in top chord increases from 0, the difference remains almost the same.

(5) As the temperature difference in bottom chord increases from negative value to 0, the difference remains almost the same.

For the deflection at midspan, w, obtained by linear solution, compared with the one obtained by nonlinear solution:

(1) As the span-to-sag ratio of top chord increases, it becomes slightly more overestimated.

(2) As the span-to-camber ratio of bottom chord increases, it becomes slightly more overestimated.

(3) As the pretension in chords increases, it becomes slightly less overestimated.

(4) As the temperature difference in top chord increases from 0, it becomes slightly more overestimated.

(5) As the temperature difference in bottom chord increases from negative value to 0, it becomes slightly less overestimated.

It is shown that, for a biconcave cable truss, the difference of resultant horizontal force in bottom chord between nonlinear and linear solutions is very sensitive to change of any of these parameters, the difference of deflection at midspan is relatively less sensitive, while the difference of resultant horizontal force in top chord keeps almost unaffected.

5.2 Biconvex Cable Truss

For the resultant horizontal force in bottom chord, H_b, obtained by linear solution, compared with the one obtained by nonlinear solution:

(1) As the span-to-camber ratio of top chord increases, it becomes slightly more underestimated.

(2) As the span-to-sag ratio of bottom chord increases, it becomes slightly more underestimated.

(3) As the pretension in chords increases, it becomes slightly less underestimated.

(4) As the temperature difference in top chord increases from negative value to 0, the difference remains almost the same.

(5) As the temperature difference in bottom chord increases from 0, it becomes slightly more underestimated.

For the resultant horizontal force in top chord, H_t, obtained by linear solution, compared with the one obtained by nonlinear solution:

(1) As the span-to-camber ratio of top chord increases, it changes from being slightly underestimated to being quite more overestimated.

(2) As the span-to-sag ratio of bottom chord increases, it becomes quite more underestimated.

(3) As the pretension in chords increases, it becomes quite less underestimated.

(4) As the temperature difference in top chord increases from negative value to 0, it becomes quite more overestimated.

(5) As the temperature difference in bottom chord increases from 0, it becomes less overestimated to some degree.

For the deflection at midspan, w, obtained by linear solution, compared with the one obtained by nonlinear solution:

(1) As the span-to-camber ratio of top chord increases, the difference remains almost the same.

(2) As the span-to-sag ratio of bottom chord increases, the difference remains almost the same.

(3) As the pretension in chords increases, the difference remains almost the same.

(4) As the temperature difference in top chord increases from negative value to 0, it becomes slightly less underestimated.

(5) As the temperature difference in bottom chord increases from 0, the difference remains almost the same.

It is shown that, for a biconvex cable truss, the difference of resultant horizontal force in top chord between nonlinear and linear solutions is very sensitive to change of any of these parameters, the difference of resultant horizontal force in bottom chord is relatively less sensitive, while the difference of deflection at midspan keeps almost unaffected.

By considering the analytical results of both types of cable truss, it is also found the increase of pretension in chords generally results in the decrease of difference between the results obtained by those two approaches.
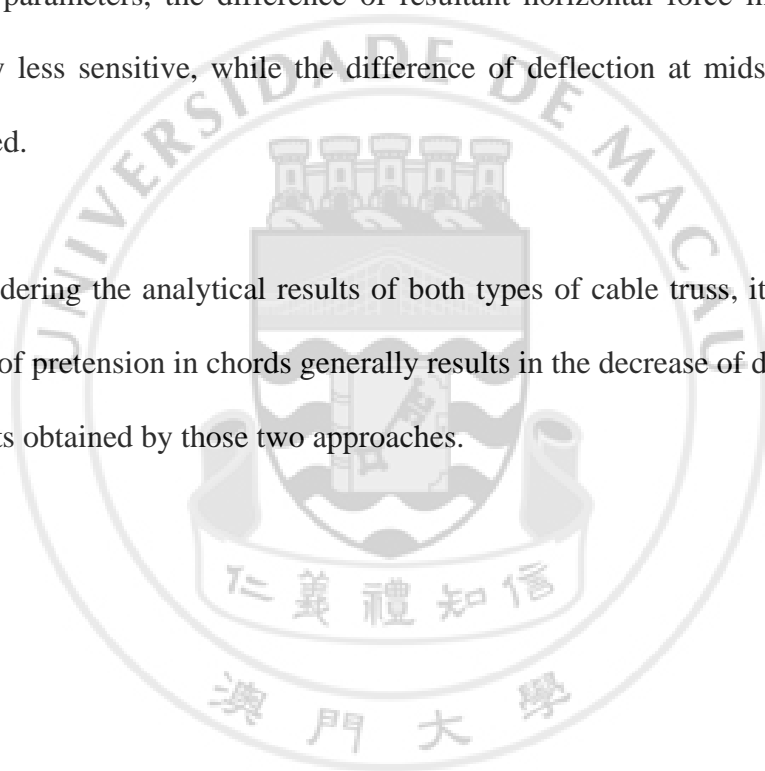
REFERENCES

Ali, H. and Abdel-Ghaffar, A. (1995), "Modeling the nonlinear seismic behavior of cable-stayed bridges with passive control bearings", *Computers and Structures*, Vol. 54, No. 3, pp. 461-492.

Andreu, A., Gil, L. and Roca, P. (2006), "A new deformable catenary element for the analysis of cable net structures", *Computers and Structures*, Vol. 84, No. 29-30, pp. 1882-1890.

Argyris, J. and Scharpf, D. (1972), "Large deflection analysis of prestressed networks", *Journal of the Structural Division*, ASCE, Vol. 98, No. ST3, pp. 633-654.

Baron, F. and Venkatesan, M.S. (1971), "Nonlinear analysis of cable and truss structures", *Journal of the Structural Division*, ASCE, Vol. 97, No. ST2, pp. 679-710.

Broughton, P. and Ndumbaro, P. (1994), *The Analysis of Cable and Catenary Structures*, Thomas Telford Services Ltd., London.

Buchholdt, H.A. (1969), "A Nonlinear Deformation Theory Applied to Two-Dimensional Pretensioned Cable Assemblies", *Proceedings*, Institution of Civil Engineers, London.

Buchholdt, H.A. (1999), *Introduction to cable roof structures*, 2nd Ed., Thomas Telford Ltd., London.

Chen, Z.H., Wu, Y.J., Yin, Y. and Shan, C. (2010), "Formulation and application of multi-node sliding cable element for the analysis of Suspen-Dome structures", *Finite Elements in Analysis and Design*, Vol. 46, No. 9, pp. 743-750.

Coyette, J. and Guisset, P. (1988), "Cable network analysis by a nonlinear programming technique", *Engineering Structures*, Vol. 10, No. 1, pp. 41-46.

Gambhir, M. and Batchelor, B. (1977), "A finite element for 3-D prestressed cablenets", *International Journal for Numerical Methods in Engineering*, Vol. 11, No. 11, pp. 1699-1718.

Gambhir, M. and Batchelor, B. (1979), "Finite element study of the free vibration of a 3-D cable networks", *International Journal of Solids and Structures*, Vol. 15, No. 2, pp. 127-136.

Gasparini, D. and Gautam, V. (2002), "Geometrically nonlinear static behavior of cable structures", *Journal of Structural Engineering*, Vol. 128, No. 10, pp. 1317-1329.

Irvine, H.M. (1981), *Cable structures*, MIT Press, Cambridge.

Jayaraman, H. and Knudson, W. (1981), "A curved element for the analysis of cable structures", *Computers and Structures*, Vol.14, No. 3-4, pp.325-333.

Kadlcak, J. (1995), *Statics of suspension cable roofs*, Balkema, Rotterdam.

Kassimali, A. and Parsi-Feraidoonian, H. (1987), "Strength of cable trusses under combined loads", *Journal of Structural Engineering*, Vol. 113, No. 5, pp. 907-924.

Kmet, S. (1994), "Rheology of pre-stressed cable structures", *Advances in Finite Element Techniques*, Papadrakakis, M. and Topping, B.H.V., Civil-Comp Press, Edinburgh, pp. 185-200.

Krishna, P. and Sparkes, S.R. (1968), "Analysis of Pretensioned Cable Systems", *Proceedings*, Institution of Civil Engineers, London.

Levy, R. and Spillers, W. (1995), *Analysis of geometrically nonlinear structures*, Kluwer Academic Publishers, London.

Mollmann, H. (1970), "Analysis of Plane Prestressed Cable Structures", *Journal of the Structural Division*, ASCE, Vol. 96, No. ST10, pp. 2059-2082.

Moskalev, N.S. (1980), *Construction of suspension roofs*, Strojizdat, Moskva.

O'Brien, W.T. and Francis, A.J. (1964), "Cable movements under two-dimensional loads", *Journal of the Structural Division*, ASCE, Vol. 90, No. ST3, pp.89-123.

Ozdemir, H. (1979), "A finite element approach for cable problems", *International Journal of Solids and Structures*, Vol. 15, No. 5, pp. 427-437.

Peyrot, A.H. and Goulois, A.M. (1978), "Analysis of flexible transmission lines", *Journal of the Structural Division*, ASCE, Vol. 104, No. ST5, pp.763-779.

Rakowski, J. (1983), "Contribution on nonlinear solution of cable systems", *Bauingenieur*, Vol. 58, No. 2, pp. 57-65.

Schleyer, F.K. (1969), *Tensile Structures*, Vol. 2, No. 4, MIT Press, Cambridge.

Such, M., Jimenez-Octavio, J.R., Carnicero, A. and Lopez-Garcia, O. (2009), "An approach based on the catenary equation to deal with static analysis of three dimensional cable structures", *Engineering Structures*, Vol. 31, No. 9, pp. 2162-2170.

Talvik, I. (2001), "Finite element modelling of cable networks with flexible supports", *Computers and Structures*, Vol. 79, No. 26-28, pp. 2443-2450.

Thornton, C.G. and Birnstiel, C. (1967), "Three-Dimensional Suspension Structures", *Journal of the Structural Division*, ASCE, Vol. 93, No. ST2, pp. 242-270.

Urelius, D.E. and Fowler, D.W. (1974), "Behaviour of pre-stressed cable truss structures", *Journal of the Structural Division*, ASCE, Vol. 100, No. ST8, pp. 1627-1641.

Wang, C., Wang, R., Dong, S. and Qian, R. (2003), "A new catenary cable element", *International Journal of Space Structures*, Vol. 18, No. 4, pp.269-275.

Yang, Y.B. and Tsay, J.Y. (2007), "Geometric nonlinear analysis of cable structures with a two-node cable element by generalized displacement control method",

International Journal of Structural Stability and Dynamics, Vol. 7, No. 4, pp. 571-588.

Zetlin, L. (1963), "Elimination of Flutter in Suspension Roofs", *Hanging Roofs*, North-Holland Publishing Co., Amsterdam.

APPENDIX A

global l Ab At Eb Et q db dt bb bt H0b H0t Leb Let LTb LTt alpha dTb dTt

l = 60; Ab = 1.3e-3; At = 2e-3;

Eb = 1.5e8; Et = 1.5e8; q = 10;

alpha = 1.2e-5;

% dTb = 0;

dTb = input('please input dTb:');

dTt = 0;

% dTt = input('please input dTt:');

% tmp = input('please input l/s:');

s = l/25;

c = l/25;

bb = 0.5;

bt = 0.5;

db = bb + s;

dt = bt + c;

H0b = 600;

% H0b = input('please input H0b:');

H0t = H0b*s/c;

DBb = db - bb; DBt = dt - bt; Hsum = H0b + H0t;

Leb = l*(1+8*(DBb/l)^2);

66

```matlab
LTb = l*(1+16/3*(DBb/l)^2);

Let = l*(1+8*(DBt/l)^2);

LTt = l*(1+16/3*(DBt/l)^2);




% ******linear solution (start)******




nb1 = Leb/(Eb*Ab) + 16*DBb^2/(3*l*Hsum);

nb2 = 16*DBb*DBt/(3*l*Hsum);

nb3 = alpha*dTb*LTb - 2*q*l*DBb/(3*Hsum);




nt1 = 16*DBb*DBt/(3*l*Hsum);

nt2 = Let/(Et*At) + 16*DBt^2/(3*l*Hsum);

nt3 = alpha*dTt*LTt - 2*q*l*DBt/(3*Hsum);




syms dHb dHt
eqn1 = nb1*dHb + nb2*dHt + nb3 ==0;
eqn2 = nt1*dHb + nt2*dHt + nt3 ==0;
[deltaHb,deltaHt]=solve([eqn1,eqn2],[dHb,dHt]);




Hb_linear = (H0b + vpa(deltaHb))/1000;

Ht_linear = (H0t - vpa(deltaHt))/1000;

w_linear = 1/(H0b+H0t) * (q*l^2/8 - vpa(deltaHb)*(db-bb) - vpa(deltaHt)*(dt-bt));




fprintf('Linear Hb = %.4f\n ',Hb_linear)
```

```matlab
fprintf('Linear Ht = %.4f\n ',Ht_linear)

fprintf('Linear w = %.4f\n ',w_linear)



% ******linear solution (end)******



% ******nonlinear solution (start)******



fun = @root2d;

x0 = [0,0];

x = fsolve(fun,x0);



Hb_nonlinear = (H0b + x(1))/1000;

Ht_nonlinear = (H0t - x(2))/1000;

w_nonlinear = 1/(H0b+x(1)+H0t-x(2)) * (q*l^2/8 - x(1)*(db-bb) - x(2)*(dt-bt));



fprintf('Nonlinear Hb = %.4f\n ',Hb_nonlinear)

fprintf('Nonlinear Ht = %.4f\n ',Ht_nonlinear)

fprintf('Nonlinear w = %.4f\n ',w_nonlinear)

fprintf('----------------------\n\n\n ')



function F = root2d(x)

global l Ab At Eb Et q db dt bb bt H0b H0t Leb Let LTb LTt alpha dTb dTt

dHb = x(1); dHt = x(2);
```

```
F(1) = 8*(db-bb)/(l^2*(H0b+dHb+H0t-dHt))*(q*l^3/12 - 2*l/3*dHb*(db-bb) -
2*l/3*dHt*(dt-bt)) ...
    + 1/(2*(H0b+dHb+H0t-dHt)^2)*(q - 8*dHb*(db-bb)/l^2 - 8*dHt*(dt-
bt)/l^2)*(q*l^3/12 - 2*l/3*dHb*(db-bb) - 2*l/3*dHt*(dt-bt)) ...
    - dHb*Leb/(Eb*Ab) - alpha*dTb*LTb;
F(2) = 8*(dt-bt)/(l^2*(H0b+dHb+H0t-dHt))*(q*l^3/12 - 2*l/3*dHb*(db-bb) -
2*l/3*dHt*(dt-bt)) ...
    - 1/(2*(H0b+dHb+H0t-dHt)^2)*(q - 8*dHb*(db-bb)/l^2 - 8*dHt*(dt-
bt)/l^2)*(q*l^3/12 - 2*l/3*dHb*(db-bb) - 2*l/3*dHt*(dt-bt)) ...
    - dHt*Let/(Et*At) - alpha*dTt*LTt;
end

% ******nonlinear solution (end)******
```